

Generalized hp -FEM for Lattice Structures*

A.W. Rüegg, A. Schneebeli[†] and R. Lauper

Research Report No. 2002-23
October 2002

Seminar für Angewandte Mathematik
Eidgenössische Technische Hochschule
CH-8092 Zürich
Switzerland

*This Research is supported under the project “Homogenization and multiple scales” HMS2000 of the EC (HPRN-CT-1999-00109), by the Swiss Federal Government under Grant BBW 01.0025-01 and by the Swiss National Science Foundation under Project “Hierarchic FE-Models for periodic lattice and honeycomb materials” with Number SNF 21-58754.99

[†]Department of Mathematics, University of Basel, Switzerland

Generalized hp -FEM for Lattice Structures*

A.W. Rüegg, A. Schneebeli[†] and R. Lauper

Seminar für Angewandte Mathematik
Eidgenössische Technische Hochschule
CH-8092 Zürich
Switzerland

Research Report No. 2002-23

October 2002

Abstract

Lattice block materials are mathematically modeled by periodic networks embedded in higher dimensional spaces. Elliptic two-scale problems on this dimensionally reduced structures are solved numerically by generalized Finite Elements. The choice of the problem adapted, conforming approximation spaces is motivated by an integral representation of the solution of the original problem extended to an infinite network with the same periodic pattern. The methods can be realized with algorithmic complexity independent of the micro scale, what is confirmed by numerical examples.

Keywords: Generalized finite element method, lattice structures, networks, homogenization, two-scale problem

*This Research is supported under the project “Homogenization and multiple scales” HMS2000 of the EC (HPRN-CT-1999-00109), by the Swiss Federal Government under Grant BBW 01.0025-01 and by the Swiss National Science Foundation under Project “Hierarchic FE-Models for periodic lattice and honeycomb materials” with Number SNF 21-58754.99

[†]Department of Mathematics, University of Basel, Switzerland

1 Introduction

Progress in manufacturing techniques allows the production of *lattice materials* of increasing complexity that are of growing importance in mechanical engineering, optoelectronics, etc.

Typically, when trying to characterize the physical properties of such materials, one has to take into account *three different length scales*: the macroscopic size l of the material block, the microscopic scale of the heterogeneities ε and finally the thickness of the bars δ . Taking the limit $\delta \rightarrow 0$, the remaining dimensionally reduced structures can be modeled by *networks* consisting of one-dimensional curves periodically arranged in a higher dimensional space. Appropriate *partial differential equations* (PDE's) describing e.g. thermal or electrical conductivity or elastic properties on networks are characterized by a highly oscillatory periodic pattern in the coefficients and geometry. Their solutions exhibit a multiple scale behaviour: a macroscopic behaviour superposed with local characteristics at micro scale length ε .

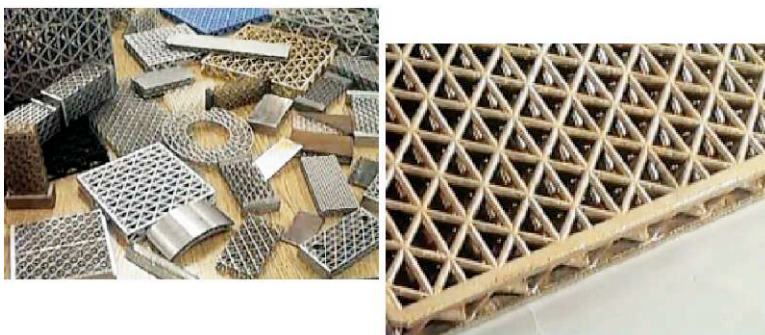


Figure 1: Periodic block lattice materials are characterized by three different length scales: the diameter l of the embedding domain Ω , the size ε of the spatial periodicity and finally the thickness of the branches δ .

The *direct numerical treatment* of such problems faces the difficulty of having to resolve microstructure. Standard Finite Element Methods (FEM) yield reliable results only with a discretization mesh with element size smaller than the smallest characteristic length scale ε of the heterogeneities. The standard FEM is therefore computationally very expensive for small ε .

Classical homogenization (see e.g. [2] for an introduction) takes a different approach to solve such problems. It tries to give an overall behaviour of the composite by neglecting the fluctuations due to the heterogeneities. A macroscopic global model (the so-called homogenized material), whose behaviour must be as close as possible to the behaviour of the composite itself. This model is derived analytically, by taking an appropriate limit as the micro length scale ε tends to zero. The obtained homogenized problem is amenable to standard

numerical treatment. However, the small scale features of the solution are lost in the homogenization process and even the computation of so-called correctors does not necessarily recover them.

In [4, 5] a high order *generalized Finite Element Method* (gFEM) for classical elliptic two-scale problems was introduced. In the present paper, a gFEM is developed for elliptic problems on periodic lattice structures. The discretization is based on two-scale *hp*-FE spaces. The standard polynomial spaces are replaced by conforming function spaces that are, in a sense, adapted to the micro-scale dependent coefficients of the differential operator, i.e. information much smaller than the macro mesh size $H \gg \varepsilon$ is built into the shape functions. These two-scale FE-spaces are obtained by augmenting the standard piecewise polynomial FE spaces with problem dependent, non-polynomial micro shape functions that reflect the correct oscillatory behaviour of the exact solution. Scale resolution by the FE mesh is not necessary.

In [6], a class of *representation formulas* for the solution of elliptic homogenization problems on unbound domains is presented. It is shown here, that the exact solutions on infinite periodic lattice structures can be represented by a Fourier-Bochner integral with respect to the lattice measure dD_x . It is proved, that the periodicity of the lattice implies *scale separation* in the generalized Fourier inversion integrals. This motivates the choice of the micro shape functions as solutions of suitable unit cell problems on the reference network.

In our gFEM-algorithm these parameter dependent unit cell problems are solved numerically with standard FEM during the start-up phase of the calculation. An analysis of the parameter dependence shows that the expensive assembly routines only have to be called one time, for any order of generalized lattice shape functions.

Taking into consideration the periodicity of the micro shape functions, the computation of the stiffness matrices to solve the discrete two scale problem can be realized with *work independent of the micro scale length ε* .

This paper is organized as follows:

Chapter 2 introduces the basic notation concerning networks and network functions that are needed to formulate the elliptic two-scale in the next chapter. The theoretical considerations in chapter 4 lead to an integral representation of the exact solution of the original problem extended to an infinite network with the same periodic pattern. This motivates the choice of the special basis functions in the gFE-discretization in chapter 5. The efficient algorithmic realization is discussed in chapter 6. Numerical experiments can be found in the last chapter. An important lemma is sourced out to appendix A because of its oblong, rather technical proof. The theorems of the theoretical section are proved in appendix B.

2 Preliminaries

In this section nomenclature of networks is introduced. A network, as a lower dimensional structure embedded in $\mathbb{R}^d, d = 2, 3$, is a set of Lebesgue measure zero. Functions on networks would vanish in standard Sobolev spaces, such as e.g. $L^2(\Omega)$ on a domain $\Omega \subset \mathbb{R}^d$. To be able to treat differential equations on networks in a variational setting, appropriate Sobolev spaces must be defined.

2.1 Networks

A one-dimensional *network* $\mathcal{N} := \bigcup_{i \in I} B_i$ is defined as a union of directed curves B_i of length $L_i > 0$ the so-called *branches* of \mathcal{N} . They are geometrically described by the parameterizations $\sigma_i : [0, L_i] \rightarrow B_i$ with respect to arc length, i.e. $B_i = \sigma_i([0, L_i])$ for all indices i in the set $I \subset \mathbb{N}$.

The endpoints $\partial B_i := \sigma_i(\{0, L_i\})$ of all branches B_i are collected in $\Gamma_{\mathcal{N}} := \bigcup_{i \in I} \partial B_i$, the set of the *nodes* of the network \mathcal{N} . It is assumed that branches only intersect at nodes, i.e. $B_i \cap B_j$ is empty or an element of $\Gamma_{\mathcal{N}}$ for all index pairs $\{i, j\} \in I \times I$.

A network \mathcal{N} is *connected* iff for every pair of nodes $(P_1, P_2) \in \Gamma_{\mathcal{N}} \times \Gamma_{\mathcal{N}}$ a connecting path along branches of \mathcal{N} exists.

The network \mathcal{N} is called *finite*, iff it consists of finitely many branches, i.e. $|I| < \infty$.

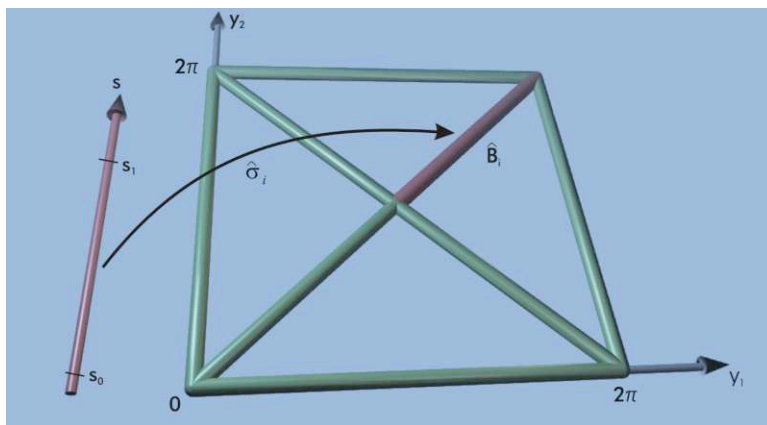


Figure 2: The network $\hat{\mathcal{N}} \subset [0, 2\pi]^2$ consists of 8 branches $\{\hat{B}_i : i = 1, \dots, 8\}$ that are geometrically determined by the parameterizations $\hat{\sigma}_i : [s_0 = 0, s_1 = \hat{L}_i] \rightarrow \mathbb{R}^2$, where \hat{L}_i is the length of the corresponding branch.

2.2 Network Functions

A \mathbb{K} -valued *network function* $u := \{u_i, i \in I\}$ on the network \mathcal{N} is given branch-wise as a sequence of functions $u_i : B_i \rightarrow \mathbb{K}$ ($\mathbb{K} = \mathbb{R}, \mathbb{C}$). Based on this definition,

function values at the nodes $\Gamma_{\mathcal{N}}$ are not uniquely defined. It will depend on the branch-wise function spaces what sort of *transmission conditions* can be imposed on functions u_i on branches with a common node.

2.3 Differentiation and Integration on Networks

For a network function u given on the network \mathcal{N} such that $u_i \circ \sigma_i \in C^1([0, L_i])$ on all branches B_i , $i \in I$ of \mathcal{N} ,

$$Du_i(\sigma_i(s)) := \frac{\partial}{\partial s} u_i(\sigma_i(s)), \quad s \in [0, L_i], \quad (1)$$

defines a new network function. The derivatives towards the nodes in ∂B_i are defined by

$$D_\nu u_i(\sigma_i(s)) := (-1)^{1-s/L_i} Du_i(\sigma_i(s)), \quad s \in \{0, L_i\}. \quad (2)$$

The corresponding integration of u over the network \mathcal{N} is defined by

$$\int_{\mathcal{N}} u(x) dD_x := \sum_{i \in I} \int_{B_i} u(x) dD_x, \quad (3)$$

where

$$\int_{B_i} u_i(x) dD_x := \int_0^{L_i} u(\sigma_i(s)) ds. \quad (4)$$

2.4 Function Spaces

The branch-wise function spaces can be reduced to the corresponding spaces on intervals.

For the network function u on the network \mathcal{N} and $k \in \mathbb{N} \cup \{\infty\}$,

$$u \in C^k(\mathcal{N}) \quad \text{iff} \quad u_i \circ \sigma_i \in C^k([0, L_i]) \quad \forall i \in I. \quad (5)$$

Equipped with the norm

$$\|u\|_{C^k(\mathcal{N})} := \sup_{i \in I} \|u_i \circ \sigma_i\|_{C^k([0, L_i])}, \quad (6)$$

$C^k(\mathcal{N})$ is a Banach space. Correspondingly for $k \in \mathbb{N}_0$ the function

$$u \in H^k(\mathcal{N}) \quad \text{iff} \quad u_i \circ \sigma_i \in H^k([0, L_i]) \quad \forall i \in I. \quad (7)$$

With the inner products

$$(u, v)_{H^k(\mathcal{N})} := \sum_{i \in I} (u_i \circ \sigma_i, v_i \circ \sigma_i)_{H^k([0, L_i])} \quad (8)$$

the defined *Sobolev spaces* become Hilbert spaces. Finally a network function

$$u \in L^\infty(\mathcal{N}) \quad \text{iff} \quad u_i \circ \sigma_i \in L^\infty([0, L_i]) \quad \forall i \in I. \quad (9)$$

The following norm is chosen

$$\|u\|_{L^\infty(\mathcal{N})} := \sup_{i \in I} \|u_i \circ \sigma_i\|_{L^\infty([0, L_i])}. \quad (10)$$

In all these definitions the topology of the branches in \mathbb{R}^d does not play any role. Therefore the spaces are isomorphic to corresponding product spaces, e.g. $L^2(\mathcal{N}) \cong \prod_{i \in I} L^2([0, 1])$. This is no longer true for the *exponentially weighted* Sobolev spaces $H_\nu^k(\mathcal{N})$, $k \in \mathbb{N}_0$, $\nu \in \mathbb{R}$: A network function

$$u \in H_\nu^k(\mathcal{N}) \quad \text{iff} \quad \|u\|_{k, \nu}^2 := \int_{\mathcal{N}} \left(\sum_{\alpha \leq k} |D_x^\alpha u(x)|^2 \right) e^{2\nu\|x\|} dD_x < \infty. \quad (11)$$

3 Two-Scale Problem

This section introduces an elliptic two-scale problem on an $2\pi\varepsilon$ -periodic network \mathcal{N}^ε embedded in a domain $\Omega \subset \mathbb{R}^d$. Typically the characteristic *micro length scale* $2\pi\varepsilon$ is in orders of magnitudes smaller than the *macro length scale* of the domain Ω , i.e. $\varepsilon \ll l = \text{diam}(\Omega)$.

The periodicity of the geometry is reflected in the rapidly oscillating coefficients representing material properties, whereas the source terms are assumed to be independent of ε .

First the computational domain is defined. Boundary and transmission conditions are needed to define a well-posed problem. Finally a variational formulation based on the Network Sobolev spaces defined in the previous section is given. The Lax-Milgram lemma shows its unique solvability.

3.1 Periodic Networks

A domain $\Omega \subset \mathbb{R}^d$ and a finite *reference network*

$$\hat{\mathcal{N}} := \bigcup_{i \in \hat{I}} \hat{B}_i \subset \hat{Y} \quad (12)$$

in the fundamental period $\hat{Y} := [-\pi, \pi]^d$ have to be chosen such that the finite $2\pi\varepsilon$ -*periodic network*

$$\mathcal{N}^\varepsilon := \mathcal{N}_\infty^\varepsilon \cap \bar{\Omega} =: \bigcup_{i \in I^\varepsilon} B_i^\varepsilon \quad (13)$$

is connected, where $\varepsilon > 0$ and the corresponding infinite network

$$\mathcal{N}_\infty^\varepsilon := \bigcup_{k \in \mathbb{Z}^d} \varepsilon(2k\pi + \hat{\mathcal{N}}). \quad (14)$$

is built of scaled, periodically arranged reference networks $\hat{\mathcal{N}}$.

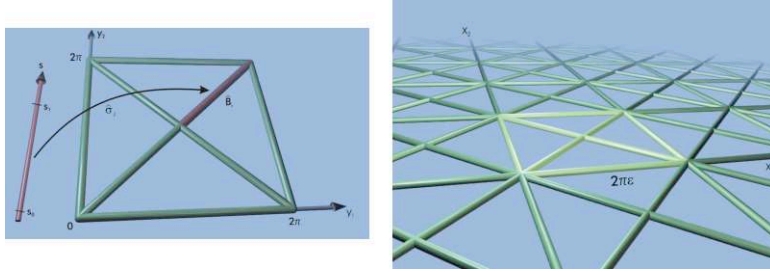


Figure 3: The infinite periodic network \mathcal{N}^ε on the right results by periodically arranging ε -scaled copies of the reference network $\hat{\mathcal{N}}$ on the left.

3.2 Diffusion Problem on \mathcal{N}^ε

On the finite periodic network \mathcal{N}^ε , the system of branch-wise given ordinary differential equations

$$L\left(\frac{x}{\varepsilon}, D_x\right) u^\varepsilon(x) := -D_x\left(A\left(\frac{x}{\varepsilon}\right) D_x u^\varepsilon(x)\right) + a\left(\frac{x}{\varepsilon}\right) u^\varepsilon(x) = f(x), \quad x \in \mathcal{N}^\varepsilon, \quad (15)$$

has to be solved for the network function u^ε , where the periodic coefficients $A, a \in L^\infty_{per}(\hat{\mathcal{N}})$ have to be *positive*, i.e. there exist constants $\gamma_A, \gamma_a > 0$ with

$$\gamma_A \leq A(y), \quad \gamma_a \leq a(y) \quad \text{for a.e. } y \in \hat{\mathcal{N}}. \quad (16)$$

To get a well-posed problem, additional conditions are needed to couple the differential equations (15). Homogeneous Dirichlet or Neumann *boundary conditions* are imposed at the intersection of the network \mathcal{N}^ε with the boundary $\partial\Omega = \Gamma_D \cup \bar{\Gamma}_N$, $\Gamma_D \cap \Gamma_N = \emptyset$ of the domain Ω :

$$u^\varepsilon|_{\Gamma_D \cap \mathcal{N}^\varepsilon} = 0 \quad (17)$$

and

$$\sum_{i \in I^\varepsilon: P \in \partial B_i^\varepsilon} A_i\left(\frac{P}{\varepsilon}\right) D_\nu u_i^\varepsilon(P) = 0 \quad \forall P \in \Gamma_{\mathcal{N}^\varepsilon} \cap \Gamma_N. \quad (18)$$

At the nodes of $\Gamma_{\mathcal{N}^\varepsilon}$ the two following *transmission conditions* hold. The solution u^ε should be uniquely defined at each node, i.e.

$$\partial B_i^\varepsilon \cap \partial B_j^\varepsilon = P \in \Gamma_{\mathcal{N}^\varepsilon} \quad \text{implies} \quad u_i(P) = u_j(P). \quad (\text{T0})$$

The energy conservation or Kirchhoff's rule

$$\sum_{i \in I^\varepsilon: P \in \partial B_i^\varepsilon} A_i\left(\frac{P}{\varepsilon}\right) D_\nu u_i^\varepsilon(P) = 0 \quad \forall P \in \Gamma_{\mathcal{N}^\varepsilon} \setminus \Gamma_N, \quad (\text{T1})$$

at all inner nodes looks equal to the homogeneous Neumann boundary conditions (18) on Γ_N .

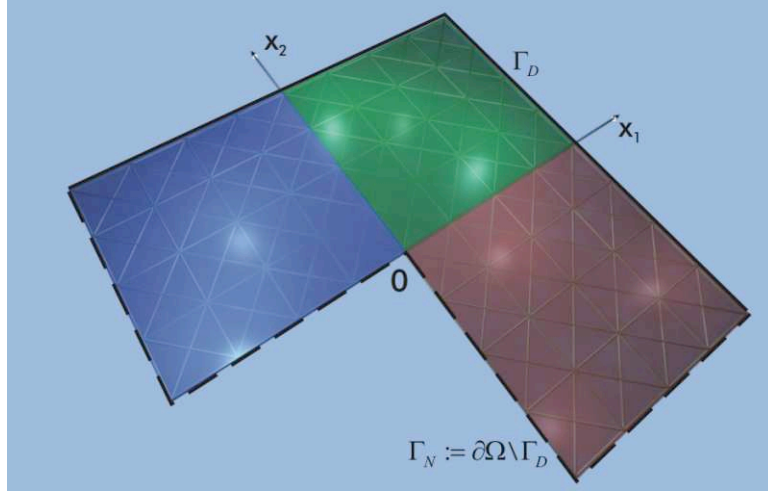


Figure 4: The computational domain \mathcal{N}^ε is determined by the intersection of the infinite network \mathcal{N}^∞ with the two-dimensional, L-shaped domain Ω . Its boundary $\partial\Omega$ consists of two parts with different boundary conditions: On Γ_D (solid) homogeneous Dirichlet (solid) are imposed, whereas the dashed lines indicate Neumann boundary conditions. $\partial\Omega$.

3.3 Variational Formulation

A variational formulation results from multiplying the differential equations (15) with a network test function v , integrating by parts and using the conditions (18) and (T1):

Find $u^\varepsilon \in \mathcal{H}_D^1(\mathcal{N}^\varepsilon)$ such that

$$\mathcal{B}^\varepsilon(u^\varepsilon, v) = (f, v)_{L^2(\mathcal{N}^\varepsilon)} \quad \forall v \in \mathcal{H}_D^1(\mathcal{N}^\varepsilon), \quad (19)$$

with right hand side f given in $L^2(\mathcal{N}^\varepsilon)$. The bilinear form $\mathcal{B}^\varepsilon : H^1(\mathcal{N}^\varepsilon) \times H^1(\mathcal{N}^\varepsilon) \rightarrow \mathbb{R}$ is defined by

$$\mathcal{B}^\varepsilon(u, v) := \int_{\mathcal{N}^\varepsilon} A\left(\frac{x}{\varepsilon}\right) D_x u(x) D_x v(x) + a\left(\frac{x}{\varepsilon}\right) u(x) v(x) dD_x. \quad (20)$$

The test and trial space

$$\mathcal{H}_D^1(\mathcal{N}^\varepsilon) := \{u \in H^1(\mathcal{N}^\varepsilon) : u|_{\Gamma_D \cap \mathcal{N}^\varepsilon} = 0, \text{ satisfying (T0)}\} \quad (21)$$

consists of branch-wise H^1 -functions that are uniquely valued at all nodes in $\Gamma_{\mathcal{N}^\varepsilon}$ and vanish on Γ_D . Due to the Sobolev lemma implying

$$H^j(B_i^\varepsilon) \hookrightarrow C^{j-1}(B_i^\varepsilon), \quad j \geq 1, \quad (22)$$

on all branches $B_i^\varepsilon, i \in I^\varepsilon$, the definition (21) makes sense.

Note the functions in $\mathcal{H}_D^1(\mathcal{N}^\varepsilon)$ are globally continuous due to the transmission

condition (T0). Because the coefficients A and a are bounded and positive, see (16), the bilinear form \mathcal{B}^ε is continuous and coercive, independent of ε . The Lax-Milgram lemma guarantees the existence and uniqueness of the solution u^ε of the variational problem (19) and yields the a priori estimate

$$\|u^\varepsilon\|_{H^1(\mathcal{N}^\varepsilon)} \leq \frac{1}{\gamma} \|f\|_{L^2(\mathcal{N}^\varepsilon)}, \quad (23)$$

with $\gamma := \min\{\gamma_A, \gamma_a\}$ is independent of ε .

4 Theory: Two-scale Problem on Infinite Network

In practice, the period $2\pi\varepsilon$ of the spatial inhomogeneities is much smaller than the dimensions of the domain Ω . Therefore, standard methods based on branch-wise discretization of the network function u^ε in (15), (19) respectively, are not feasible due to their computational expense.

Motivated by [4, 5], a generalized Finite Element Method (gFEM) is developed which uses two-scale FE-spaces with $2\pi\varepsilon$ -periodic, problem-dependent shape functions to capture the correct oscillatory behavior of the solution. The choice of the micro shape functions is motivated by a generalized Fourier-Bochner integral representation first proposed in [6] of the exact solution of the original problem extended here to an *infinite periodic network*.

4.1 Representation Formula

Adapting the ideas of [6], a representation formula of the exact solution u_∞^ε of

$$L\left(\frac{x}{\varepsilon}, D_x\right) u_\infty^\varepsilon(x) = f(x), \quad x \in \mathcal{N}_\infty^\varepsilon, \quad (24)$$

satisfying (T0), (T1),

on the infinite periodic network $\mathcal{N}_\infty^\varepsilon$ is based on the *Fourier transform* of the network function $f \in L^2(\mathcal{N}_\infty^\varepsilon)$ that equals the right hand side of (19) on \mathcal{N}^ε and vanishes on $\mathcal{N}_\infty^\varepsilon \setminus \mathcal{N}^\varepsilon$. For functions $F \in H^1(\mathbb{R}^d)$ with

$$f = F|_{\mathcal{N}_\infty^\varepsilon}. \quad (25)$$

the standard Fourier transform

$$\hat{F}(t) := \frac{1}{(2\pi)^{d/2}} \int_{\mathbb{R}^d} F(x) e^{-it \cdot x} dx, \quad t \in \mathbb{R}^d, \quad (26)$$

is well defined. The additional regularity of F guarantees that the restriction (25) makes sense, at least in the two-dimensional case.

Theorem 1 (*Trace theorem for network functions*)

Let $\mathcal{N}_\infty^\varepsilon$ be an infinite periodic network given by (14) that consists of Lipschitz continuous branches, i.e. the geometry of the corresponding reference network $\hat{\mathcal{N}}$ is defined by parameterizations $\sigma_i \in C^{0,1}(L_i), i \in \hat{I}$.

Then the trace operator is a continuous linear map from $H^1(\mathbb{R}^2)$ to $L^2(\mathcal{N}_\infty^\varepsilon)$ such that

$$\|u|_{\mathcal{N}_\infty^\varepsilon}\|_{L^2(\mathcal{N}_\infty^\varepsilon)} \leq C(\hat{\mathcal{N}}) \max\{\varepsilon, \frac{1}{\varepsilon}\} \|u\|_{H^1(\mathbb{R}^2)} \quad (27)$$

holds for all $u \in H^1(\mathbb{R}^2)$ with a constant $C(\hat{\mathcal{N}})$ only depending on the geometry of $\hat{\mathcal{N}}$.

This follows from the standard trace theorem for H^1 -functions on Lipschitz domains combined with a scaling argument.

Due to the linearity of the equation, the ansatz

$$u_\infty^\varepsilon(x) = \frac{1}{2\pi} \int_{\mathbb{R}^2} \hat{F}(t) \psi(x, t) dt, \quad x \in \mathcal{N}_\infty^\varepsilon \quad (28)$$

for u_∞^ε in (24) leads to the parameter dependent problem

$$L\left(\frac{x}{\varepsilon}, D_x\right) \psi(x, t) = e^{it \cdot x}, \quad x \in \mathcal{N}_\infty^\varepsilon, t \in \mathbb{R}^2, \quad (29)$$

(T0), (T1) hold,

that should be solved by the kernel $\psi(\cdot, t)$. As some sort of fundamental solution, it is the response of the micro structure to a wave with wave vector $t \in \mathbb{R}^2$. Unlike e.g. asymptotic homogenization, the kernel $\psi(x, t)$ also incorporates responses to high frequency 'volume' sources as arise in dynamic simulations.

Note that the restriction of $e^{it \cdot x}$ in (29) onto the infinite network $\mathcal{N}_\infty^\varepsilon$ is not in $L^2(\mathcal{N}_\infty^\varepsilon)$, but $\|e^{it \cdot x}\|_{L^2_{-\nu}(\mathcal{N}_\infty^\varepsilon)}, \nu > 0$ is finite. Therefore

Find $\psi \in \mathcal{H}_{-\nu}^1(\mathcal{N}_\infty^\varepsilon)$ such that

$$\Psi^\varepsilon(\psi, v) = \langle \psi, e^{it \cdot x} \rangle_{(\mathcal{H}_\nu^1(\mathcal{N}_\infty^\varepsilon))^* \times \mathcal{H}_\nu^1(\mathcal{N}_\infty^\varepsilon)} \quad \forall v \in \mathcal{H}_\nu^1(\mathcal{N}_\infty^\varepsilon) \quad (30)$$

is an appropriate variational formulation of (29) for right hand sides in the dual space of

$$\mathcal{H}_\nu^1(\mathcal{N}_\infty^\varepsilon) := \{u \in H_\nu^1(\mathcal{N}_\infty^\varepsilon) : (T0) \text{ is satisfied}\} \quad (31)$$

with the sesquilinear form $\Psi^\varepsilon : H_{-\nu}^1(\mathcal{N}_\infty^\varepsilon) \times H_\nu^1(\mathcal{N}_\infty^\varepsilon) \rightarrow \mathbb{C}$ defined for $\nu \geq 0$ by

$$\Psi^\varepsilon(u, v) := \int_{\mathcal{N}_\infty^\varepsilon} A\left(\frac{x}{\varepsilon}\right) D_x u(x) \overline{D_x v(x)} + a\left(\frac{x}{\varepsilon}\right) u(x) \overline{v(x)} dD_x. \quad (32)$$

For $\nu = 0$, the coercivity and continuity of Ψ^ε would imply unique solvability of the equation (30) by the Lax-Milgram lemma as in the previous section. A perturbation argument can be employed to verify

Theorem 2 (*inf-sup*)

There exist constants $C, \nu_0, \gamma > 0$ independent of ε such that for all $\nu \in (0, \nu_0)$, $\varepsilon > 0$

$$(i1) \quad |\Psi^\varepsilon(u, v)| \leq C \|u\|_{1, -\nu} \|v\|_{1, \nu} \quad \forall u \in H_{-\nu}^1(\mathcal{N}_\infty^\varepsilon), v \in H_\nu^1(\mathcal{N}_\infty^\varepsilon) \quad (\text{Continuity})$$

$$(i2) \quad \inf_{\|u\|_{1, -\nu}=1} \sup_{\|v\|_{1, \nu}=1} |\Psi^\varepsilon(u, v)| \geq \gamma \quad (\text{Inf-sup condition})$$

$$(i3) \quad \sup_{u \in H_{-\nu}^1(\mathcal{N}_\infty^\varepsilon)} |\Psi^\varepsilon(u, v)| > 0 \quad \forall v \in H_\nu^1(\mathcal{N}_\infty^\varepsilon) \setminus \{0\} \quad (\text{Injectivity})$$

The statements of the previous theorem are exactly the properties required by the Bakuška-Brezzi theory [1] to guarantee existence and uniqueness of the solution u of (30) under the assumption that $\nu \in (0, \nu_0)$ for all $\varepsilon > 0$. Additionally, the a-priori estimate

$$\|u\|_{H_{-\nu}^1(\mathcal{N}_\infty^\varepsilon)} \leq \frac{1}{\gamma} \|f\|_{(H_\nu^1(\mathcal{N}_\infty^\varepsilon))^*} \quad (33)$$

holds with $\gamma := \min\{\gamma_A, \gamma_a\}$ independent of ε .

To get the estimate (33) in the case of (29) independent of t and fixed ν , the following theorem is of interest. With regard to later considerations, this general setting is chosen.

Theorem 3 (*Analyticity of $t \mapsto e^{it \cdot x}$*)

The mapping

$$\mathcal{D}_{\nu_2} \ni t \mapsto G(t) := e^{it \cdot x} \in (H_\nu^1(\mathcal{N}_\infty^\varepsilon))^* \quad (34)$$

is holomorphic in $\mathcal{D}_{\nu_2} := \{t \in \mathbb{C}^2 : \|Imt\|_\infty < \nu_2\}$, $\nu_2 := \frac{\nu}{2\sqrt{2}}$ with values in the Banach space $(H_\nu^1(\mathcal{N}_\infty^\varepsilon))^*$.

Additionally, $G_k(t) := (ix)^k e^{it \cdot x} \in (H_\nu^1(\mathcal{N}_\infty^\varepsilon))^*$ is the $k \in \mathbb{N}^2$ -th partial derivative of $G(t)$ and

$$\|G_k\|_{(H_\nu^1(\mathcal{N}_\infty^\varepsilon))^*} \leq C(\hat{\mathcal{N}}, \varepsilon, \nu) \frac{2}{\pi} \left(\frac{2}{\nu}\right)^{\|k\|_1+1} (\|k\|_1 + 1)! \quad (35)$$

with $C(\hat{\mathcal{N}}, \varepsilon, \nu) = C(\hat{\mathcal{N}}) e^{(2+\frac{1}{\sqrt{2}})\pi\varepsilon\nu} \sqrt{\pi\nu + \varepsilon^{-1}}$ and $\|x\|_1 := |x_1| + |x_2|$.

The properties of the map $t \mapsto e^{it \cdot x}$ shown in the previous theorem together with the existence and uniqueness statements of the linear problem (29, 30) lead to

Theorem 4 (*Analyticity of $t \mapsto \psi(\cdot, t)$*)

For $t \in \mathcal{D}_{\nu_2}$ with $\nu_2 := \frac{\nu_0}{2\sqrt{2}}$ the mapping

$$t \mapsto \psi(\cdot, t) \in H_{-\nu}^1(\mathcal{N}_\infty^\varepsilon) \quad (36)$$

is holomorphic in \mathcal{D}_{ν_2} with values in the Banach space $H_{-\nu}^1(\mathcal{N}_\infty^\varepsilon)$. Moreover, $\psi_k(t) \in H_{-\nu}^1(\mathcal{N}_\infty^\varepsilon)$ defined as the solution of

$$\Psi^\varepsilon(\psi_k(t), v) = \langle G_k(t), v \rangle, \quad \forall v \in \mathcal{H}_\nu^1(\mathcal{N}_\infty^\varepsilon) \quad (37)$$

equals

$$\psi_k(t) = D_t^k \psi(\cdot, t) = \partial_{t_1}^{k_1} \partial_{t_2}^{k_2} \psi(\cdot, t) \quad (38)$$

for all $k \in \mathbb{N}^2$ and

$$\|\psi_k(t)\|_{1, -\nu} \leq \frac{C(\hat{\mathcal{N}}, \varepsilon, \nu)}{\gamma} \frac{2}{\pi} \left(\frac{2}{\nu}\right)^{\|k\|_1 + 1} (\|k\|_1 + 1)! \quad (39)$$

where γ is the inf-sup constant from theorem 2 and

$$C(\hat{\mathcal{N}}, \varepsilon, \nu) = C(\hat{\mathcal{N}}) e^{\left(2 + \frac{1}{\sqrt{2}}\right) \pi \varepsilon \nu} \sqrt{\pi \nu + \varepsilon^{-1}}$$

as in the previous theorem.

Towards to the verification of the representation formula, the result is first proved under the assumption that the Fourier transform of the right hand side of (24) has compact support. The general case will follow by an appropriate limiting process.

For $F \in L^2(\mathbb{R}^2)$ and $M > 0$ define F_M as the inverse Fourier transform of

$$\hat{F}_M(t) := \mathbf{1}_{\|t\| \leq M} \hat{F}(t), \quad t \in \mathbb{R}^2, \quad (40)$$

i.e.

$$F_M(x) := \frac{1}{2\pi} \int_{\mathbb{R}^2} \hat{F}_M(t) e^{it \cdot x}, \quad x \in \mathbb{R}^2, \quad (41)$$

and denote by $u_M^\varepsilon \in H_{-\nu}^1(\mathcal{N}_\infty^\varepsilon)$ the correspondingly truncated integral

$$u_M^\varepsilon(x) = \frac{1}{2\pi} \int_{\mathbb{R}^2} \hat{F}_M(t) \psi(x, t) dt, \quad x \in \mathcal{N}_\infty^\varepsilon. \quad (42)$$

This integral has to be interpreted as a Bochner integral (see [3]) over $\Omega_M := \{t \in \mathbb{R}^2 : \|t\| \leq M\}$ of a $H_{-\nu}^1(\mathcal{N}_\infty^\varepsilon)$ -valued function. In order to show that the integral really has such a mathematical meaning, a sequence of finitely-valued functions $\{w_M^n(\cdot, t) : n \in \mathbb{N}\}$ on \mathbb{R}^2 has to be found for each $M > 0$, such that

$$(bi1) \quad \lim_{n \rightarrow \infty} \|\hat{F}_M(t) \psi(\cdot, t) - w_M^n(\cdot, t)\|_{1, -\nu} = 0 \quad \text{for a.e. } t \in \Omega_M,$$

$$(bi2) \quad \lim_{n \rightarrow \infty} \int_{\mathbb{R}^2} \|\hat{F}_M(t) \psi(\cdot, t) - w_M^n(\cdot, t)\|_{1, -\nu} dt = 0 \quad \text{for a.e. } t \in \Omega_M.$$

The equation (bi1) expresses the strong measurability of the integrand $\hat{F}_M(t) \psi(\cdot, t)$ and implies that the positive, real-valued functions $t \mapsto \|\hat{F}_M(t) \psi(\cdot, t)\|_{1, -\nu}$, $t \mapsto \|\hat{F}_M(t) \psi(\cdot, t) - w_M^n(\cdot, t)\|_{1, -\nu}$ respectively are Lebesgue-measurable. Therefore the integrals in (bi2) are well-defined and the Bochner integral of $\hat{F}_M(t) \psi(\cdot, t)$ over $\Omega_M \subset \mathbb{R}^2$ is defined by the limes

$$\int_{\Omega_M} \hat{F}_M(t) \psi(\cdot, t) dt := \lim_{n \rightarrow \infty} \int_{\Omega_M} w_M^n(\cdot, t) dt \quad \text{in } H_{-\nu}^1(\mathcal{N}_\infty^\varepsilon). \quad (43)$$

The integrals of the simple functions on the right hand side are defined in a standard way by finite sums. Their limes in $H_{-\nu}^1(\mathcal{N}^{\varepsilon_\infty})$ exists: Because of the inequality

$$\begin{aligned} \left\| \int_{\Omega_M} w_M^{n_1}(\cdot, t) dt - w_M^{n_2}(\cdot, t) dt \right\|_{1, -\nu} &\leq \int_{\Omega_M} \|\hat{F}_M(t)\psi(\cdot, t) - w_M^{n_1}(\cdot, t)\|_{1, -\nu} \\ &+ \int_{\Omega_M} \|\hat{F}_M(t)\psi(\cdot, t) - w_M^{n_2}(\cdot, t)\|_{1, -\nu}, \end{aligned}$$

the sequence $\{\int_{\Omega_M} w_M^n(\cdot, t) dt : n \in \mathbb{N}\} \subset H_{-\nu}^1(\mathcal{N}_\infty^\varepsilon)$ is Cauchy and the completeness of the Banach space guarantees the existence of its limes.

The existence of such a sequence $\{w_M^n(\cdot, t) : n \in \mathbb{N}\}$ on \mathbb{R}^2 for each positive M is essential and constructed in the proof of

Theorem 5 (*Simple functions*)

For $M, \varepsilon > 0$ and $t \mapsto \psi(\cdot, t)$ continuous it exists a sequence $\{w_M^n(\cdot, t)\} \subset H_{-\nu}^1(\mathcal{N}_\infty^\varepsilon)$ of finitely-valued functions with the properties (bi1) and (bi2).

The continuity of $\psi(\cdot, t)$ is ensured by theorem 4.

Using the notation introduced in the proof of theorem 5 $u_M^\varepsilon \in \mathcal{H}_{-\nu}^1(\mathcal{N}_\infty^\varepsilon)$ defined in (42) can be written as

$$u_M^\varepsilon(x) = \lim_{n \rightarrow \infty} \frac{1}{2\pi} \sum_{j=1}^{J_n} \hat{F}_M(t_M^{k,j}) \psi(x, t_M^{k,j}) |\Omega_M^{n,j}|, \quad x \in \mathcal{N}_\infty^\varepsilon. \quad (44)$$

Is this the solution of (30) with corresponding right hand side f_M ? A positive answer is given by

Theorem 6 (*Integral representation: $M < \infty$*)

For each $\varepsilon, M > 0$

$$\Psi^\varepsilon(u_M^\varepsilon, v) = \int_{\mathcal{N}_\infty^\varepsilon} f_M(x) \overline{v(x)}$$

holds for all $v \in \mathcal{H}_\nu^1(\mathcal{N}_\infty^\varepsilon)$.

Note that the restrictions to the network are well defined because $F_M(x)$ and F are in $H^1(\mathbb{R}^2)$.

A combination of the statement of the previous theorem with (29), (30) respectively leads to

$$\|u_\infty^\varepsilon - u_M^\varepsilon\|_{1, -\nu} \leq \frac{1}{\gamma} \|F - F_M\|_{L^2(\mathcal{N}_\infty^\varepsilon)} \quad (45)$$

and using that $F \in H^1(\mathbb{R}^2)$ with the trace theorem and the Parseval's equality, to get

$$\begin{aligned}
\|u_\infty^\varepsilon - u_M^\varepsilon\|_{1,-\nu} &\leq \frac{C(\varepsilon)}{\gamma} \|F - F_M\|_{H^1(\mathbb{R}^2)} \\
&\leq \frac{C(\varepsilon)}{\gamma} \|(1 + |t|^2)^{1/2}(\hat{F} - \hat{F}_M)\|_{L^2(\mathbb{R}^2)} \\
&\leq \frac{C(\varepsilon)}{\gamma} \left(\int_{\mathbb{R}^2 \setminus \Omega_M} (1 + |t|^2) |\hat{F}(t)|^2 \right)^{1/2} \\
&\rightarrow 0, \quad \text{as } M \rightarrow \infty,
\end{aligned} \tag{46}$$

the following theorem is obvious.

Theorem 7 (*Integral representation: $M \rightarrow \infty$*)

Let $F(x) \in H^1(\mathbb{R}^2)$, $\nu \in (0, \nu_0)$, $\varepsilon > 0$ and further $u_\infty^\varepsilon \in \mathcal{H}^1(\mathcal{N}_\infty^\varepsilon)$ solving the symmetric variational formulation of (29) on $\mathcal{N}_\infty^\varepsilon$. Then, as an element of the weighted Sobolev space $H_{-\nu}^1(\mathcal{N}_\infty^\varepsilon) \supset H^1(\mathcal{N}_\infty^\varepsilon)$, u_∞^ε admits the Fourier-Bochner integral representation

$$u_\infty^\varepsilon(x) = \frac{1}{2\pi} \int_{\mathbb{R}^2} \hat{F}(t) \psi(x, t) dt, \quad x \in \mathcal{N}_\infty^\varepsilon. \tag{47}$$

Note that the previously presented results are valid in a very general *in particular non-periodic* setting, whereas the next section is focussed on the periodic two-scale problems.

Stronger regularity assumptions on F in (25) allow the extension of (47) to dimension $d = 3$.

4.2 Scale Separation

Following [6], the periodicity of the coefficients allows the scale separation of the kernel $\psi(x, \varepsilon, t)$ into a product of Fourier waves $e^{it \cdot x}$ with periodic, highly oscillatory functions $\phi\left(\frac{x}{\varepsilon}, \varepsilon, t\right)$ encoding the fast scale of the problem, i.e

$$\psi(x, \varepsilon, t) = e^{it \cdot x} \phi\left(\frac{x}{\varepsilon}, \varepsilon, t\right). \tag{48}$$

Here ϕ solves the *unit cell problem* on $\hat{\mathcal{N}}$ with $t \in \mathbb{C}^2$, $\varepsilon > 0$:

Find $\phi(\cdot, \varepsilon, t) \in \mathcal{H}_{\text{per}}^1(\hat{\mathcal{N}})$ such that

$$\Phi_t^\varepsilon(\phi, v) = \varepsilon^2 \int_{\hat{\mathcal{N}}} \overline{v(y)} dD_y \quad \forall v \in \mathcal{H}_{\text{per}}^1(\hat{\mathcal{N}}), \tag{49}$$

where the sesquilinear form $\Phi_t^\varepsilon : H_{\text{per}}^1(\hat{\mathcal{N}}) \times H_{\text{per}}^1(\hat{\mathcal{N}}) \rightarrow \mathbb{C}$ is defined by

$$\Phi_t^\varepsilon(u, v) := \int_{\hat{\mathcal{N}}} A(y) D_y(u(y) e^{it \cdot \varepsilon y}) \overline{D_y(v(y) e^{it \cdot \varepsilon y})} + \varepsilon^2 a(y) u(y) \overline{v(y)} dD_y, \tag{50}$$

and the Sobolev space

$$\mathcal{H}_{per}^1(\hat{\mathcal{N}}) := \{u \in H_{per}^1(\hat{\mathcal{N}}) : (\text{T0}) \text{ is satisfied}\}. \quad (51)$$

Summarizing:

Theorem 8 (*Scale separation*)

Let $F \in H^1(\mathbb{R}^2)$, $\nu \in (0, \nu_0)$ and $\varepsilon > 0$. Then, as an element of the weighted Sobolev space $\mathcal{H}_{-\nu}^1(\mathcal{N}_\infty^\varepsilon)$, the solution u_∞^ε of the symmetric variational formulation of (29) admits the Bochner integral representation (47) with the kernel ψ defined by (48) in which the periodic function ϕ solves the unit cell problem (49).

5 Generalized FE-Discretization

Because the kernel $\phi(y, \varepsilon, t)$ solving the unit cell problem (49) is analytic in the Fourier vector t , the Fourier-Bochner integral (28) can be approximated by the finite sum

$$\mathbf{1}_{[-\frac{\pi}{h}, \frac{\pi}{h}]^2} \frac{h^2}{2\pi} \sum_{k \in \mathbb{Z}_N^2} \hat{f}(kh) \phi\left(\frac{x}{\varepsilon}, \varepsilon, kh\right) e^{ikh \cdot x}, \quad (52)$$

where for $N \in \mathbb{N}$

$$\mathbb{Z}_N^2 := \{k \in \mathbb{Z}^2 : |k_i| \leq N, p = 1, 2\}$$

and $h \sim N^{-\frac{1}{2}}$. For the problem class considered in [4, 5] the approximation error decays exponentially in N , independent of ε , for analytic data f . The micro scale of the solution can be already resolved by $\text{span}\{\phi(\cdot, \varepsilon, t) : t \in T\}$, i.e. the unit cell problem (49) has to be solved for only finitely many wave vectors $t \in T$, $|T| =: \hat{\mu} < \infty$. The macroscopic behaviour of the solution, represented by the Fourier waves, is approximated by standard $H_D^1(\Omega)$ -conforming, piecewise polynomial FE-spaces on the computational domain $\Omega \subset \mathbb{R}^2$.

5.1 Numerical Computation of the Micro Shape Functions

The computation of the micro shape functions $\phi(y, \varepsilon, t)$, $y \in \hat{\mathcal{N}}$ includes two steps:

- (i) The unit cell problem (49) on $\hat{\mathcal{N}}$ is solved numerically for $|\hat{\mu}| \gg \mu$ different parameters $t \in T \subset \mathbb{C}^d$. (*Oversampling*)
- (ii) A well-conditioned basis is extracted via singular value decomposition (SVD) of the matrix consisting of the solution vectors from (i). (*Orthogonalization*)

Due to the analyticity of the kernel $\phi(\cdot, \varepsilon, t)$ with respect to the frequency t , its evaluations at the collocation points $t \in T$ are almost linear dependent. The orthogonalization (ii) is needed to obtain a better-conditioned basis without changing the space. The omission of the $\hat{\mu} - \mu$ “non-essential” micro functions can be viewed as *principal component analysis* on the fine scale.

5.1.1 Discrete Unit Cell Problem

The infinite dimensional test and trial space $\mathcal{H}_{per}^1(\hat{\mathcal{N}})$ in the unit cell problem (49) is replaced by the finite dimensional subspace

$$\mathcal{S}_{per}^{\hat{p},1}(\hat{\mathcal{N}}, \hat{\tau}) := \{u \in \mathcal{H}_{per}^1(\hat{\mathcal{N}}) : u_i \in S^{\hat{p}_i,1}(\hat{B}_i, \hat{\tau}_i), i \in \hat{I}\}, \quad (53)$$

of the globally continuous network functions that belong branch-wise to the hp -FE spaces

$$S^{p,1}(B, \tau) := \{u \in H^1(B) : \deg(u|_K) = p_K, K \in \tau\}, \quad (54)$$

where $\tau = \{K_j : j \in J\}$ is a mesh consisting of open intervals of a finite partition of B , i.e. $B = \bigcup_{j \in J} K_j$ and $i \neq j$ implies $K_i \cap K_j = \emptyset$.

With $\hat{N} := \dim(\mathcal{S}_{per}^{\hat{p},1}(\hat{\mathcal{N}}, \hat{\tau}))$ and the basis

$$\{\hat{v}_i(y) : i = 1, \dots, \hat{N}\} \quad (55)$$

of (53), the matrix $C := [c_1(\varepsilon), \dots, c_{\hat{\mu}}(\varepsilon)]$ collects column-wise the coefficient vectors $c_j(\varepsilon)$ of the solutions $\tilde{\phi}_j(y) = c_j(\varepsilon)^T \hat{\underline{v}}(y)$ of the discrete unit cell problem (49) for the $\hat{\mu}$ different parameters $t_j \in T$.

5.1.2 Basis Reduction at the ε -Scale

Without changing the space $\text{span}\{\tilde{\phi}_j(y) : j = 1, \dots, \hat{\mu}\} \subset \mathcal{H}_{per}^1(\hat{\mathcal{N}})$, the singular value decomposition

$$C = U \text{diag}(\sigma_1, \dots, \sigma_{\hat{\mu}}) V^T \quad (56)$$

orthogonalized the coefficient vectors. Finally

$$\phi_j\left(\frac{x}{\varepsilon}\right) := U_j^T \hat{\underline{v}}\left(\frac{x}{\varepsilon}\right), \quad j = 1, \dots, \hat{\mu}. \quad (57)$$

defines the periodic micro shape functions ϕ . The micro spaces

$$\mathcal{M}_\varepsilon^\mu := \text{span}\{\phi_j\left(\frac{x}{\varepsilon}\right) : j = 1, \dots, \mu + 1\} \subset \mathcal{H}_{per}^1(\varepsilon\hat{\mathcal{N}}), \quad (58)$$

and

$$\mathcal{M}_\varepsilon^0 := \text{span}\{1\}, \quad (59)$$

are generated by the micro shape functions $\phi_j\left(\frac{x}{\varepsilon}\right)$ corresponding to the leading singular values $\sigma_j, j = 1, \dots, \mu + 1$, where $\mu \ll \hat{\mu}$ in (58) is chosen such that $\sigma_j < \delta$ for all $\mu < j < \hat{\mu}$. Here δ is a truncation parameter specified by the user. For δ of the order of machine precision, the number of basis functions is reduced substantially, while the change in span is negligible.

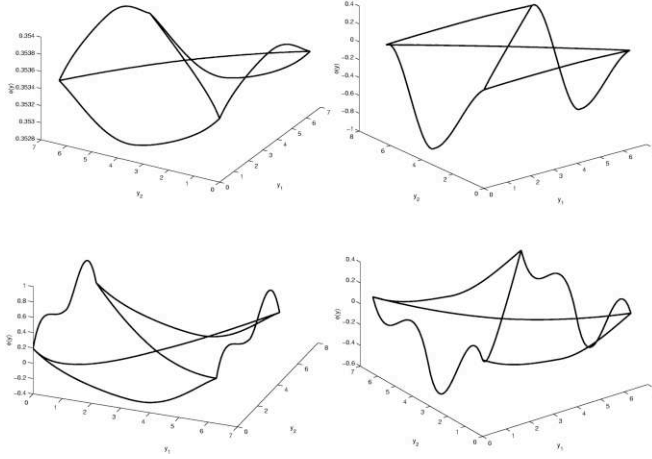


Figure 5: The dominant micro basis functions $\phi_j(y), j = 0, \dots, 3$ for data given in the last section.

5.2 Generalized FE-Spaces

Remembering the scale separation of the approximated solution (52) in form of a finite sum of products of the previously constructed, highly oscillating micro scale shape functions ϕ with analytic Fourier waves,

$$\mathcal{S}_D^{p,\mu,1}(\Omega, \tau) := \{u \in \mathcal{H}_D^1(\mathcal{N}^\varepsilon) : u|_K \in F_K(\mathcal{P}^{p_K}(\tilde{K})) \otimes \mathcal{M}_\varepsilon^{\mu_K}, K \in \tau\} \quad (60)$$

is an obvious choice for a conforming two-scale discretization space, based on an ε -independent macro triangulation $\tau = \{K_j : j \in J\}$ of the two-dimensional domain Ω covering the network \mathcal{N}^ε . For each element $K \in \tau$, a basis of the space $\mathcal{P}^{p_K}(\tilde{K})$ of all polynomials of total degree p_K on the reference element $\tilde{K} = (0, 1)^2$ is transported by the element map $F_K : \tilde{K} \rightarrow K$ onto K in the physical domain. Similarly to the vector $\{p_K, K \in \tau\}$ of the element-wise polynomial p_K , a vector $\{\mu_K, K \in \tau\}$ collects the number μ_K of micro scale basis functions chosen on elements $K \in \tau$.

6 Algorithmic Aspects

For fixed parameter $\varepsilon > 0$, given geometry Ω and data, the overall algorithm

Algorithm 1 (*Main Algorithm*)

- $hpFEM(A, a, \hat{\tau}, \hat{p}, \varepsilon, t) \quad \forall t \in T \hookrightarrow C = [c_1(\varepsilon), \dots, c_{\hat{\mu}}(\varepsilon)]$
- $SVD(C, \delta) \hookrightarrow \mathcal{M}_\varepsilon^\mu$
- $microQuad(\mathcal{M}_\varepsilon^\mu) \hookrightarrow Q_\varepsilon^\mu$

- $UnitCell = (Q_\varepsilon^\mu, [\hat{\tau}, \dots])$
- $gFEM_{UnitCell}(A, a, \tau, p, \mu) \hookrightarrow u_N$

decomposes basically into two main parts: The unit cell computations on the reference network $\hat{\mathcal{N}}$ that define the interface $UnitCell$ containing informations needed by the generalized EM to solve the main problem on $\mathcal{N}^\varepsilon \subset \overline{\Omega}$ with work independent of ε . To achieve this goal, the so-called micro quadratures play a key rule. The corresponding function $microQuad$ precomputes the moments

$$(Q_\varepsilon^\mu)_{\mathcal{A},u,v,du,dv}^{r,s,i,j} := \int_{\hat{\mathcal{N}}} y_1^r y_2^s \dot{y}_1^i \dot{y}_2^j \mathcal{A}(y) D_y^{du} \phi_u(y) D_y^{dv} \phi_v(y) dD_y, \quad (61)$$

with $\mathcal{A} \in \{A, a\}$, the derivatives $\dot{y}(\sigma(s)) := \frac{\partial}{\partial s} \sigma(s)$ and indices

$$r, s \in \{0, 1, \dots, p_{max}\}, \quad u, v \in \{1, 2, \dots, \mu_{max}\}, \quad i, j, du, dv \in \{0, 1\}.$$

The field Q_ε^μ allows for efficient evaluation of stiffness matrix and load vector in $gFEM$. But first, the unit cell problem has to be solved for $\hat{\mu} = |T|$ different parameters $t \in T$. An analysis of the t -dependence of the sesquilinear form Φ_t^ε in (49) leads to an optimized algorithmic realization of the first step in main algorithm.

6.1 Unit Cell Computations

The unit cell problem (49) is discretized via hp -FE spaces (53) on appropriate meshes $\hat{\tau}$.

6.1.1 Parameter Dependence

There is no reason to change the approximation space depending on the parameter $t \in T$. Therefore it is desirable to call the assembly routine with its expensive quadrature rules only once. The decomposition

$$\begin{aligned} \{\Phi_t^\varepsilon(\hat{v}_k, \hat{v}_l)\}_{k,l} &= M_{A,1,1}^{0,0} - i\varepsilon(\bar{t} \cdot \begin{bmatrix} M_{A,1,0}^{1,0} \\ M_{A,1,0}^{0,1} \end{bmatrix} - t \cdot \begin{bmatrix} M_{A,0,1}^{1,0} \\ M_{A,0,1}^{0,1} \end{bmatrix}) \\ &+ \varepsilon^2(t \cdot \begin{bmatrix} M_{A,0,0}^{1,1} & M_{A,0,0}^{1,2} \\ M_{A,0,0}^{2,1} & M_{A,0,0}^{2,2} \end{bmatrix} \cdot \bar{t} + M_{a,0,0}^{0,0}), \end{aligned} \quad (62)$$

of the sesquilinear form Φ_t^ε from (50) into a sum of vector components of t multiplied by parameter independent matrices

$$\{M_{\mathcal{A},u,v}^{i,j}\}_{k,l} := \int_{\hat{\mathcal{N}}} \dot{y}_1^i \dot{y}_2^j \mathcal{A}(y) D_y^u \hat{v}_k D_y^v \overline{\hat{v}_l} dD_y, \quad (63)$$

enables the decoupling of the assembly process from the iteration over $t \in T$. This is shown in

Algorithm 2 (*Unit Cell Computations*)

- $\forall i \in \hat{I}$:
 - $\forall K \subset \hat{B}_i$:
 - $M_{A,u,v}^{i,j} = assemble(K)$
- $\forall t \in T$:
 - $C \leftrightarrow [C, (M_{A,1,1}^{0,0} - i\varepsilon(\bar{t}_1 M_{A,1,0}^{1,0} + \bar{t}_2 M_{A,1,0}^{0,1}) + \dots)^{-1} b]$
 - $\mathcal{M}_\varepsilon^\mu \leftrightarrow SVD(C, \delta)$

For every pass of this second loop a linear system has to be solved numerically. The resulting coefficient vector extends the matrix C by one column.

6.1.2 Assembly on Periodic Meshes

To build the matrices (63), the function *assemble* in algorithm 2 has to map local degrees of freedoms corresponding to shape functions living on the reference interval onto global ones such that the resulting global basis functions are continuous. Instead of assembling branch-wise and imposing afterwards the constraints needed to satisfy the transmission condition (T0) between the branches, it is more natural to prevent such separation. The connectivity is realized by nodes that are represented by zero-dimensional topological objects and elements defined by two nodes and an element map. Realized by this hierarchic data structures, the reference network becomes toric because of its periodic boundaries. In this general setting the assembly procedure already used for the homogenization problems in [7] also works on networks in \mathbb{R}^d , $d = 2, 3$.

6.2 Efficient Integration of the Micro Shape Functions

The function *gFEM* computes the solution u_N of the macro problem (19) in the discrete gFE-space $\mathcal{S}_D^{p,\mu,1}(\Omega, \tau)$. If the elements $K \in \tau$ are rectangles with $m_1, m_2, M_1, M_2 \in \mathbb{N}$ such that

$$K = 2\pi\varepsilon(m_1, m_1 + M_1) \times (m_2, m_2 + M_2), \quad (64)$$

the work to evaluate the stiffness matrix entries is independent of M_1, M_2 and ε .

Let $\{\nu_i(x) : i \in I\}$ be a tensor product basis of the piecewise polynomial space $S^{p,1}(\Omega, \tau)$ (see e.g. [8]), i.e. the factorization

$$\nu_i(x) = \nu_{i_1}(x_1)\nu_{i_2}(x_2) \quad (65)$$

of the shape functions holds. The evaluation of the bilinear form $\mathcal{B}^\varepsilon(\nu_i\phi_u, \nu_j\phi_v)$ for the two-scale basis functions $\{\nu_i(x)\phi_u(\frac{x}{\varepsilon})\}_{i,u}$ on $K^- := 2\pi\varepsilon[m_1, m_1 + M_1] \times$

$[m_2, m_2 + M_2)$ equals

$$\int_{\mathcal{N}^\varepsilon \cap K^-} A\left(\frac{x}{\varepsilon}\right) D_x \left[\nu_{i_1}(x_1) \nu_{i_2}(x_2) \phi_u\left(\frac{x}{\varepsilon}\right) \right] D_x \left[\nu_{j_1}(x_1) \nu_{j_2}(x_2) \phi_v\left(\frac{x}{\varepsilon}\right) \right] dD_x. \quad (66)$$

Because $D_x \nu(x) = \dot{x} \nabla_x \nu(x)$ with $\dot{x}(\sigma(s)) := \frac{\partial}{\partial s} \sigma(s)$ on all branches of \mathcal{N}^ε , the integral (66) decomposes into a sum of terms

$$\int_{\mathcal{N}^\varepsilon \cap K^-} \dot{x}_1^{d_1} \dot{x}_2^{d_2} [\nu_{i_1}^{(d_{i_1})} \nu_{j_1}^{(d_{j_1})}](x_1) [\nu_{i_2}^{(d_{i_2})} \nu_{j_2}^{(d_{j_2})}](x_2) [\mathcal{A} \phi_u \phi_v] \left(\frac{x}{\varepsilon} \right) dD_x, \quad (67)$$

where $\mathcal{A} \in \{A, a\}$, di, dj, du, dv indicate orders of differentiation and for shorter notation set $d_1 := d_{i_1} + d_{j_1}$, $d_2 := d_{i_2} + d_{j_2}$. The substitution $\tilde{x} := \varepsilon^{-1}(x - r)$ leads to

$$c^\varepsilon \int_{\tilde{\mathcal{N}} \cup \tilde{K}^-} \dot{x}_1^{d_1} \dot{x}_2^{d_2} [\nu_{i_1}^{(d_{i_1})} \nu_{j_1}^{(d_{j_1})}](x_1(\tilde{x}_1)) [\nu_{i_2}^{(d_{i_2})} \nu_{j_2}^{(d_{j_2})}](x_2(\tilde{x}_2)) [\mathcal{A} \phi_u \phi_v](\tilde{x}) dD_{\tilde{x}}, \quad (68)$$

with $c^\varepsilon = \varepsilon^{1-d_1-d_2-du-dv}$, the transformed element $\tilde{K}^- := [0, 2\pi M_1) \times [0, 2\pi M_2)$ and $\tilde{\mathcal{N}} := \varepsilon^{-1}(\mathcal{N}^\varepsilon - r)$. Using the periodicity of $\mathcal{A} \phi_u \phi_v$ and the monomial expansions of the shape functions

$$\nu_i^{(d)}(y) = \sum_{r=0}^{deg(\nu_i)-d} c_r^{i,d} y^r, \quad d \in \mathbb{N}_0, \quad (69)$$

the integral finally writes

$$c^\varepsilon \sum_{r_i, r_j} c_{r_i}^{i_1, d_{i_1}} c_{r_j}^{j_1, d_{j_1}} \sum_{s_i, s_j} c_{s_i}^{i_2, d_{i_2}} c_{s_j}^{j_2, d_{j_2}} \sum_{p=0}^{r_i+r_j} \binom{r_i+r_j}{p} (2\pi)^{r_i+r_j-p} S_{M_1}^{r_i+r_j-p} \sum_{q=0}^{s_i+s_j} \binom{s_i+s_j}{q} (2\pi)^{s_i+s_j-p} S_{M_2}^{s_i+s_j-q} (Q_\varepsilon^\mu)_{\mathcal{A}, u, v, du, dv}^{r, s, di, dj}. \quad (70)$$

The tensor Q_ε^μ results from the unit cell computations. The sum of powers

$$S_M^k := \sum_{l=1}^{M-1} l^k, \quad M, k \in \mathbb{N} \quad (71)$$

of natural numbers can be expressed in terms of tabulated Bernoulli numbers b_n

$$\sum_{l=1}^m l^k = \frac{m^{k+1}}{k+1} + \frac{m^k}{2} + \frac{1}{2} \binom{k}{1} b_2 m^{k-1} + \frac{1}{4} \binom{k}{3} b_4 m^{k-3} + \frac{1}{6} \binom{k}{5} b_6 m^{k-5} + \dots, \quad (72)$$

ending with a term containing either m or m^2 .

Runtime and memory can be saved by take into consideration symmetries of the high dimensional tensors appearing in the calculations. Sum factorization techniques are applied to implement the loops efficiently.

7 Numerical Results

Based on the reference network geometry consisting of six branches that form a diagonal cross in a frame, two numerical examples are considered: A periodic network in a L-shaped domain and the situation of a local defect. Apart from the solutions $u_N(x)$, the fluxes $A(\frac{x}{\varepsilon})D_x u_N(x)$ are also of interest. Time measurements proof the calculation time is really independent of ε as predicted in the previous section.

7.1 Unit Cell

The data on the reference network in Fig.(2) are defined in global coordinates: The diffusion coefficient is

$$A(y_1, 0) = \sin(y_1) + 2 \quad \text{and} \quad A(0, y_2) = \sin(y_2) + 2 \quad (73)$$

on $\partial\hat{Y}$ and

$$A(y) = y_1 + y_2 + 1 \quad (74)$$

on the inner branches of $\hat{\mathcal{N}}$, where the reaction coefficient $a(y) = 3$. On the outer branches

$$a(y_1, 0) = a(0, y_2) = 2. \quad (75)$$

Based on this data, the micro scale shape functions in Fig.(5) result. They are used in the two following problems with polynomial right hand side $f(x) = x_1 + 2x_2$ on the corresponding computational domain $\Omega \subset \mathbb{R}^2$.

7.2 L-shaped Domain

The problem (19) is solved numerically on an L-shaped domain Ω for $\varepsilon = \frac{1}{12\pi}$. Fig.(4) shows the boundary conditions imposed on $\partial\Omega$. The mesh consists of 12 square elements with side lengths $\frac{1}{4}$. They result from a subdivision of the initial mesh with three squares located in the three quadrants. Choosing $p = \mu = 4$ uniformly for all elements, the lattice problem consisting of about 450 single branches is solved for u_N with only 480 degrees of freedom. This number is even independent of ε as it is shown in the next example.

7.3 Local Defect

The second numerical example simulates the situation of a local defect in a periodic network covered by the unit square. Therefore the computational domain Ω with the boundary conditions is given in Fig.(8). Reducing the micro length scale from $\frac{1}{40\pi}$ to $\frac{1}{80\pi}$, the number of single branches increase substantially to almost 1600 branches, whereas the dimension of the discrete problem and the resolution quality do not change.

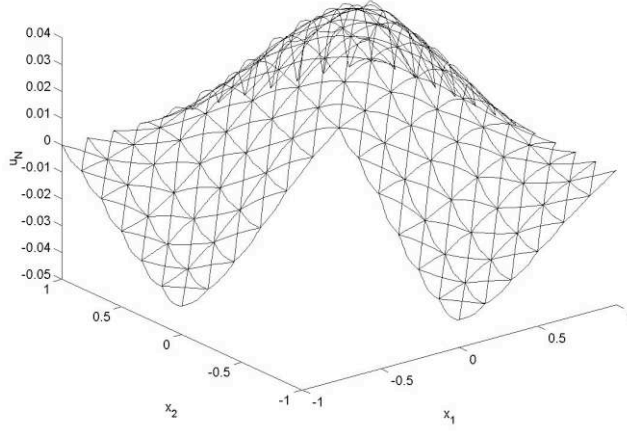


Figure 6: Solution $u_N(x)$.

7.4 CPU-time

To show that the computational cost is independent of the micro scale, CPU-times for solving the first example are plotted against ε . The blue line which denotes the overall time implies an ε -dependance. But these measurements also include the time needed to write the data for graphical post processing to hard-disk. The red line, indicated with "HDD-Space" shows the amount of graphics data depending on ε .

Finally the almost constant green line results from measurements stopped right before the data files are written. It confirms the theoretical predictions: The work does not depend on ε .

A Properties of the Exponential Function

The following lemma is essential for the proofs of the theorems in appendix B.

Lemma 1 For $t \in \mathcal{D}_{\frac{\nu}{2\sqrt{2}}}$, $\nu > 0$ the inequality

$$\|x^k e^{it \cdot x}\|_{0, -\nu}^2 \leq C(\hat{\mathcal{N}}) \left[\frac{2}{\pi} \left(\frac{2}{\nu} \right)^{\|k\|_1 + 1} (\|k\|_1 + 1)! \right]^2 e^{\pi \varepsilon \nu (\sqrt{2} + 4)} \left(\pi \nu + \frac{1}{\varepsilon} \right). \quad (76)$$

holds with $C(\hat{\mathcal{N}})$ only depending on the geometry of the reference network.

Proof. The inequality

$$|x_1^{k_1} x_2^{k_2} e^{it \cdot x}|^2 \leq |x_1|^{2k_1} |x_2|^{2k_2} e^{\frac{\nu}{\sqrt{2}} \|x\|_1} \quad (77)$$

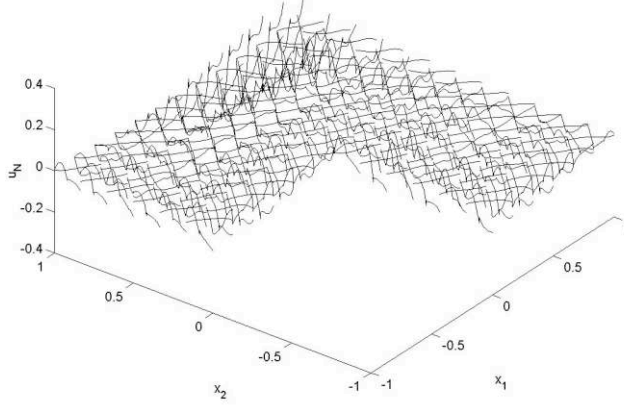


Figure 7: Flux $A(\frac{x}{\varepsilon})D_x u_N(x)$.

and the "radial" decomposition of the infinite index set $2\mathbb{Z}^2$

$$2\mathbb{Z}^2 = \bigcup_{r \in \mathbb{N}} \{z \in \mathbb{Z}^2 : |z_i| = 2r, i \in \{1, 2\}\} =: R_r, \quad (78)$$

where for all $x \in \mathcal{N}_r^\varepsilon := \bigcup_{z \in R_r} \varepsilon(\pi z + \hat{\mathcal{N}})$, $r \in \mathbb{N}$,

- $|R_r| = \begin{cases} 1, & r = 0 \\ 8r, & r \neq 0 \end{cases}$
- $\varepsilon\pi(2r - 1) \leq |x_i| \leq \varepsilon\pi(2r + 1), \quad i = 1, 2,$
- $\varepsilon\pi(2r - 1) \leq \|x\| \leq \varepsilon\pi\sqrt{2}(2r + 1)$

hold, lead to

$$\begin{aligned} \|x^k e^{it \cdot x} e^{-\nu \|x\|}\|_0^2 &\leq \int_{\mathcal{N}_\infty^\varepsilon} |x|^{2k} e^{\frac{\nu}{\sqrt{2}} \|x\|} e^{-2\nu \|x\|} dD_x \\ &\leq \sum_{r \in \mathbb{N}} \int_{\mathcal{N}_r^\varepsilon} |x|^{2k} e^{\frac{\nu}{\sqrt{2}} \|x\|} e^{-2\nu \|x\|} dD_x \\ &\leq \sum_{r \in \mathbb{N}} 8r \varepsilon C(\hat{\mathcal{N}}) (\varepsilon\pi(2r + 1))^{2\|k\|_1} e^{\frac{\nu}{\sqrt{2}} 2\pi\varepsilon(2r+1)} e^{-2\nu\varepsilon\pi(2r-1)} \\ &\leq 8\varepsilon C(\hat{\mathcal{N}}) (\varepsilon\pi)^{2\|k\|_1} e^{\pi\varepsilon\nu(\sqrt{2}+2)} \sum_{r \in \mathbb{N}} r(2r + 1)^{2\|k\|_1} e^{-2\pi\varepsilon\nu r(2-\sqrt{2})} \\ &\leq 8\varepsilon C(\hat{\mathcal{N}}) (\varepsilon\pi)^{2\|k\|_1} e^{\pi\varepsilon\nu(\sqrt{2}+2)} 4^{\|k\|_1} \sum_{r \in \mathbb{N}} (r + 1)^{2\|k\|_1+1} e^{-2\pi\varepsilon\nu r} \end{aligned}$$

with $C(\hat{\mathcal{N}}) := |\hat{I}| \max\{L_i : i \in \hat{I}\}$ representing the reference cell geometry. The last estimate follows, considering

$$r(2r + 1)^{2\|k\|_1} e^{-2\varepsilon\nu r(2-\sqrt{2})} \leq 4^{\|k\|_1} (r + 1)^{2\|k\|_1+1} e^{-2\pi\varepsilon\nu r}. \quad (79)$$

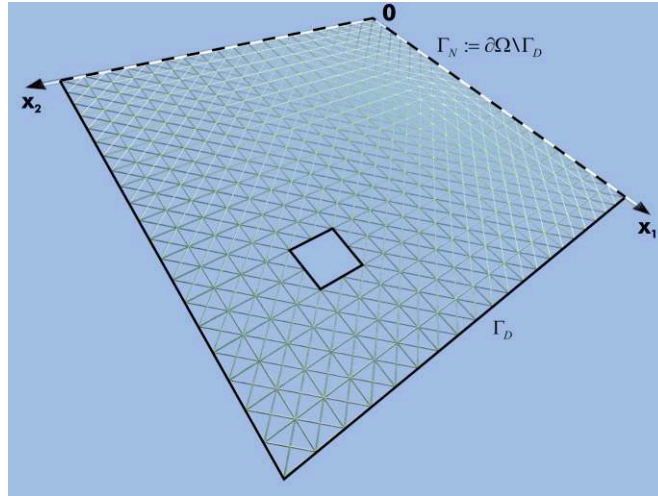


Figure 8: The situation of a problem with a local defect. The homogeneous boundary conditions are indicated as follows: dashed means Neumann, sold stands for Dirichlet.

It remains to discuss the sum

$$\sum_{n \in \mathbb{N}} n^a e^{-bn} = \int_0^{\infty} \varphi(x) dx, \quad (80)$$

with the positive constants $a = 2\|k\|_1 + 1$ and $b = 2\pi\varepsilon\nu$ and the function $\varphi(x) := \sum_{n \in \mathbb{N}} h(n)\chi_{(n-1, n]}(x)$ interval wise given by $h(x) := x^a e^{-bx}$. Since

$$\left(\frac{a}{eb}\right)^a = h\left(\frac{a}{b}\right) \quad (81)$$

is the maximal value of h , the function φ is overestimated by

$$\tilde{h}(x) := \begin{cases} \left(\frac{a}{eb}\right)^a, & 0 \leq x < \frac{a}{b} + 1 \\ h(x), & x > \frac{a}{b} + 1 \end{cases}, x \in \mathbb{R}^+, \quad (82)$$

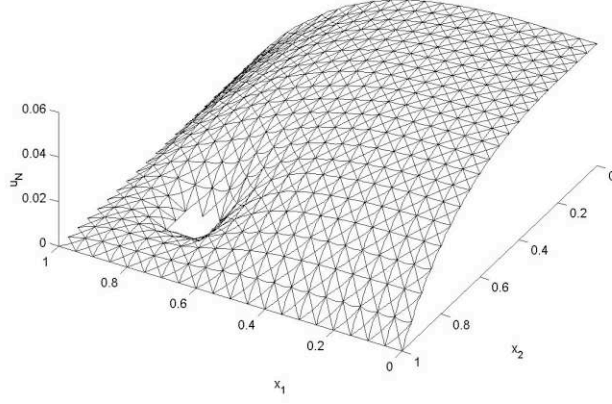


Figure 9: Solution $u_N(x)$.

and therefore

$$\begin{aligned}
\int_0^\infty \varphi(x) dx &\leq \left(\frac{a}{b} + 1\right) \left(\frac{a}{eb}\right)^a + \int_{\frac{a}{b}+1}^\infty h(x) dx \\
&\leq \left(\frac{a}{b} + 1\right) \left(\frac{a}{eb}\right)^a + \int_0^\infty h(x) dx \\
&\leq \left(\frac{a}{b} + 1\right) \left(\frac{1}{b}\right)^a a! + \left(\frac{1}{b}\right)^{a+1} a! \\
&\leq \left(\frac{1}{b}\right)^{a+1} a! a \left(1 + \frac{b+1}{a}\right) \\
&\leq \left(\frac{1}{b}\right)^{a+1} a! a(2+b)
\end{aligned} \tag{83}$$

holds because of Stirling's formula

$$n! = \sqrt{2\pi n} \left(\frac{n}{e}\right)^n e^{s_n} \quad \text{with} \quad \frac{1}{12n + \frac{2}{5n}} < s_n < \frac{1}{12n} \tag{84}$$

and the inequality $\frac{b+1}{a} \leq b+1$ with $a \leq 1$ used to verify the last step. Re-substituting the original variables of a and b and applying the estimate

$$(2\|k\|_1 + 1)!(2\|k\|_1 + 1) \leq [2(\|k\|_1 + 1)]! \leq 4^{\|k\|_1+1} ((\|k\|_1 + 1)!)^2. \tag{85}$$

leads to

$$\|x^k e^{it \cdot x}\|_{0,-\nu}^2 \leq C(\hat{\mathcal{N}}) \left[\frac{2}{\pi} \left(\frac{2}{\nu}\right)\right]^{\|k\|_1+1} ((\|k\|_1 + 1)!)^2 e^{\pi\varepsilon\nu(\sqrt{2}+4)} \left(\pi\nu + \frac{1}{\varepsilon}\right).$$

□

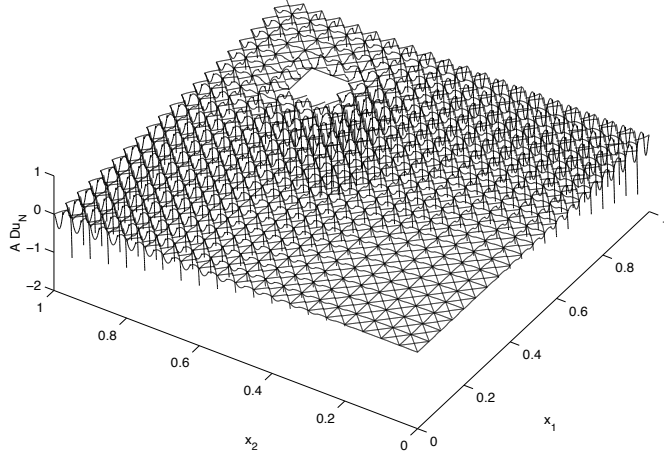


Figure 10: Flux $A(\frac{x}{\epsilon})D_x u_N(x)$.

B Proofs of the Theorems

This section collects the proofs of all the theorems.

B.1 Proof of Theorem 1

The standard trace theorem for H^1 -functions on Lipschitz domains is used followed by a scaling argument.

For each branch \hat{B}_i of the reference network $\hat{\mathcal{N}}$ a two-dimensional Lipschitz domain $\hat{\Omega}_i \subset \hat{Y}$ can be found with $\hat{B}_i \subset \partial\hat{\Omega}_i$. As a consequence, $u \in H^1(\hat{Y})$ fulfils

$$\|u|_{\hat{\mathcal{N}}}\|_{L^2(\hat{\mathcal{N}})}^2 \leq C(\hat{\mathcal{N}})\|u\|_{H^1(\hat{Y})}^2 \quad (86)$$

with the only geometry dependent constant $C(\hat{\mathcal{N}})$ due to the trace theorem for H^1 -functions on Lipschitz domain.

Scaling down this inequality by the factor ε leads to the estimate

$$\|u\|_{L^2(\varepsilon\hat{\mathcal{N}})}^2 \leq \max\{\varepsilon, \frac{1}{\varepsilon}\}C(\hat{\mathcal{N}})\|u\|_{H^1(\varepsilon\hat{Y})}^2 \quad (87)$$

for $u \in H^1(\varepsilon\hat{Y})$. Therefore

$$\begin{aligned} \|u|_{\mathcal{N}_\infty^\varepsilon}\|_{L^2(\mathcal{N}_\infty^\varepsilon)}^2 &\leq \sum_{k \in \mathbb{Z}^2} C(\hat{\mathcal{N}}) \max\{\varepsilon, \frac{1}{\varepsilon}\} \|u\|_{H^1(\varepsilon(2\pi k + \hat{Y}))}^2 \\ &\leq C(\hat{\mathcal{N}}) \max\{\varepsilon, \frac{1}{\varepsilon}\} \|u\|_{H^1(\mathbb{R}^2)}^2 \end{aligned} \quad (88)$$

holds if $u \in H^1(\mathbb{R}^2)$.

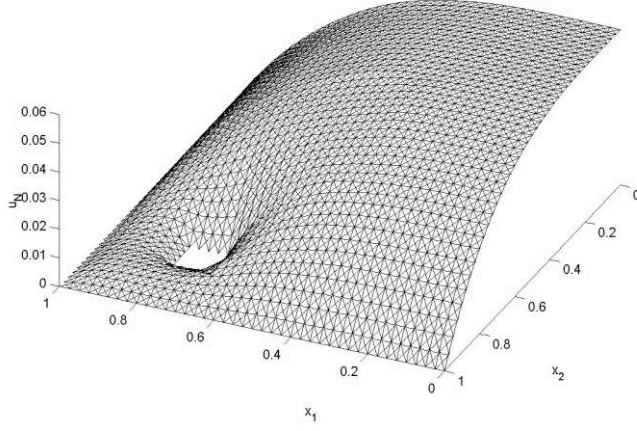


Figure 11: Solution $u_N(x)$.

B.2 Proof of Theorem 2

The continuity (i1) of the sesquilinear form applied to $u \in H_{-\nu}^1(\mathcal{N}_\infty^\varepsilon)$ and $v \in H_\nu^1(\mathcal{N}_\infty^\varepsilon)$ is obvious because

$$\begin{aligned}
|\Psi^\varepsilon(u, v)| &\leq \|A\|_\infty \int_{\mathcal{N}_\infty^\varepsilon} |D_x u(x) e^{-\nu\|x\|} \overline{D_x v(x) e^{\nu\|x\|}}| dD_x \\
&\quad + \|a\|_\infty \int_{\mathcal{N}_\infty^\varepsilon} |u(x) e^{-\nu\|x\|} \overline{v(x) e^{\nu\|x\|}}| dD_x \\
&\leq \max\{\|A\|_\infty, \|a\|_\infty\} (\|D_x u\|_{0, -\nu} \|D_x v\|_{0, \nu} + \|u\|_{0, -\nu} \|v\|_{0, \nu}) \\
&\leq \max\{\|A\|_\infty, \|a\|_\infty\} \|u\|_{1, -\nu} \|v\|_{1, \nu}.
\end{aligned}$$

To prove the inf-sub condition (i2) it is sufficient to show the existence of $\nu_0, \gamma, C > 0$ independent of ε such that for each $u \in C_0^\infty(\mathcal{N}_\infty^\varepsilon)$ exists $v_u \in H_\nu^1(\mathcal{N}_\infty^\varepsilon)$ fulfilling

$$(i2.1) \quad \|v_u\|_{1, \nu} \leq C \|u\|_{1, -\nu}$$

$$(i2.2) \quad |\Psi^\varepsilon(u, v_u)| \geq \gamma \|u\|_{1, -\nu}^2.$$

Since $C_0^\infty(\mathcal{N}_\infty^\varepsilon) := \{u \in C^\infty(\mathcal{N}_\infty^\varepsilon) : \text{supp } u \subset\subset \mathbb{R}^2\}$ is dense in $H_{-\nu}^1(\mathcal{N}_\infty^\varepsilon)$, the inf-sup condition follows.

Let $u \in C_0^\infty(\mathcal{N}_\infty^\varepsilon)$ arbitrary, fixed and define $v_u(x) := u(x) e^{-2\nu\|x\|}$ for $\nu > 0$. Obviously $v_u \in H_\nu^1(\mathcal{N}_\infty^\varepsilon)$ and

$$\begin{aligned}
\|v_u\|_{1, \nu}^2 &= \int_{\mathcal{N}_\infty^\varepsilon} (|u(x)|^2 + |D_x u(x) - 2\nu \frac{x}{\|x\|} \cdot \dot{x} u(x)|^2) e^{-2\nu\|x\|} dD_x \\
&\leq \|u\|_{0, -\nu}^2 + \|D_x u\|_{0, -\nu}^2 + 4\nu \|D_x u\|_{0, -\nu} \|u\|_{0, -\nu} + 4\nu^2 \|u\|_{0, -\nu}^2,
\end{aligned}$$

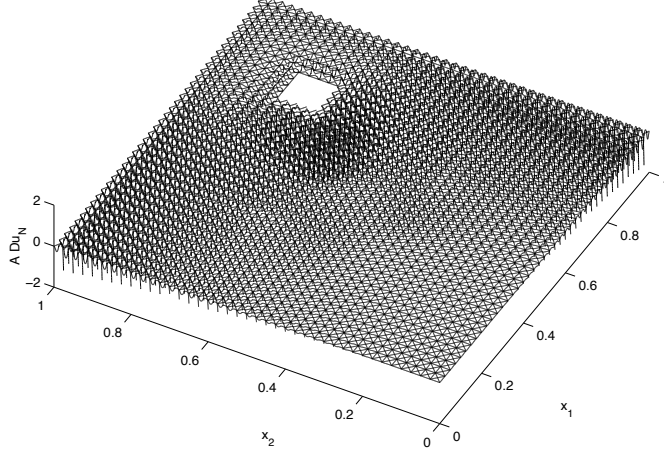


Figure 12: Flux $A(\frac{x}{\varepsilon})D_x u_N(x)$.

where $|D_x||x| = |\frac{x}{|x|} \cdot \dot{x}| \leq \frac{|x|}{|x|} |\dot{x}| = 1$ is applied. This only holds due to the parameterizations with respect to arc length.

The inequality $(a+b)^2 \leq 2(a^2+b^2)$, $a, b \in \mathbb{R}$ motivates

$$\begin{aligned} \|v_u\|_{1,\nu}^2 &\leq \|u\|_{0,-\nu}^2 + 2\|D_x u\|_{0,-\nu}^2 + 8\nu^2\|u\|_{0,-\nu}^2 \\ &\leq \max\{2, 1 + 8\nu^2\}\|u\|_{1,-\nu}^2. \end{aligned}$$

Therefore (i2.1) holds with $C = \sqrt{\max\{2, 1 + 8\nu^2\}}$ independent of ε .

Based on the coercivity of Ψ^ε for arguments in $H^1(\mathcal{N}_\infty^\varepsilon)$, i.e $\nu = 0$, a perturbation argument is used to show (i2.2) for $0 < \nu < \nu_0$:

$$\begin{aligned} \Psi^\varepsilon(u, v_u) &= \int_{\mathcal{N}_\infty^\varepsilon} \left\{ A\left(\frac{x}{\varepsilon}\right) |D_x u(x)|^2 + a\left(\frac{x}{\varepsilon}\right) |u(x)|^2 \right\} e^{-2\nu|x|} dD_x \\ &\quad - 2\nu \int_{\mathcal{N}_\infty^\varepsilon} A\left(\frac{x}{\varepsilon}\right) D_x u(x) \overline{u(x)} \frac{x}{|x|} \cdot \dot{x} e^{-2\nu|x|} dD_x \\ &=: \Psi_1^\varepsilon(u) - \nu \Psi_2^\varepsilon(u). \end{aligned} \tag{89}$$

The estimate

$$|\Psi_1^\varepsilon(u)| \geq \min\{\gamma_A, \gamma_a\} \|u\|_{1,-\nu} \tag{90}$$

with the positive constants γ_A, γ_a from (16), and

$$\begin{aligned} |\Psi_2^\varepsilon(u)| &\leq 2\|A\|_\infty \int_{\mathcal{N}_\infty^\varepsilon} |D_x u(x)| |u(x)| e^{-2\nu|x|} dD_x \\ &\leq \|A\|_\infty (\|u\|_{0,-\nu}^2 + \|D_x u\|_{0,-\nu}^2) \end{aligned} \tag{91}$$

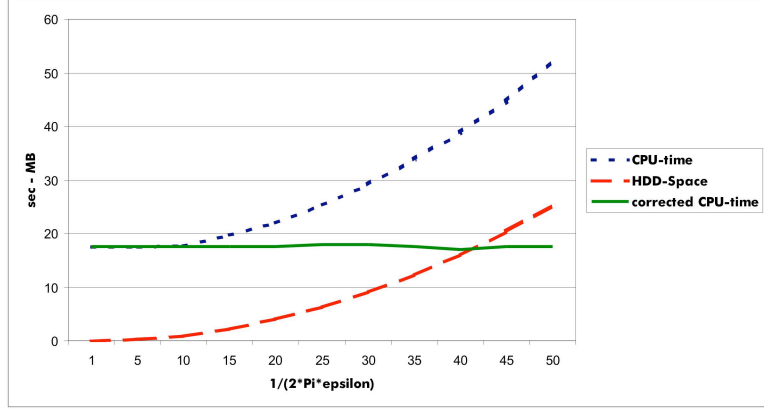


Figure 13: Independence of the solution time of the micro scale parameter ε .

lead to the inequality

$$\begin{aligned} |\Psi^\varepsilon(u, v_u)| &\geq |\Psi_1^\varepsilon(u)| - \nu |\Psi_2^\varepsilon(u)| \\ &\geq (\min\{\gamma_A, \gamma_a\} - \nu \|A\|_\infty) \|u\|_{1, -\nu}^2, \end{aligned} \quad (92)$$

which proves (i2.2) with $0 < \nu_0 < \frac{\min\{\gamma_A, \gamma_a\}}{\|A\|_\infty}$ and $\gamma = \min\{\gamma_A, \gamma_a\} - \nu \|A\|_\infty$ independent of ε .

It remains to show the injectivity property (i3) that basically works in the same way as the proof of the inf-sup condition: For each $v \in H_\nu^1(\mathcal{N}_\infty^\varepsilon) \setminus \{0\}$ and the definition $u_v(x) := v(x)e^{2\nu\|x\|} \in H_{-\nu}^1(\mathcal{N}_\infty^\varepsilon)$ the inequality

$$|\Psi^\varepsilon(u_v, v)| \geq (\min\{\gamma_A, \gamma_a\} - \nu \|A\|_\infty) \|v\|_{1, \nu}^2 > 0 \quad (93)$$

holds for the same reason as (92) if $0 \leq \nu < \nu_0$.

B.3 Proof of Theorem 3

A Taylor expansion at $t \in \mathcal{D}_{\nu_2}$ in the axis-aligned differentiation direction $e_k, k \in \{1, 2\}$ leads to

$$\begin{aligned} &\left| \frac{1}{h} \langle G(t + he_k) - G(t) - G_{e_k}(t), v \rangle_{(H_\nu^1(\mathcal{N}_\infty^\varepsilon))^* \times H_\nu^1(\mathcal{N}_\infty^\varepsilon)} \right| \\ &\leq h \|e^{it \cdot x} \left(\frac{(ix_k)^2}{2!} + h \frac{(ix_k)^3}{3!} + h^2 \frac{(ix_k)^4}{4!} + \dots \right)\|_{0, -\nu} \|v\|_{1, \nu} \end{aligned} \quad (94)$$

for each $v \in H_\nu^1(\mathcal{N}_\infty^\varepsilon)$ and $h > 0$. The lemma in appendix A ensures that the terms $\|x^k e^{it \cdot x}\|_{0, -\nu}$ are bounded and taking the limit $h \rightarrow 0$ proves the first statement. Analogously works the proof for higher order derivatives.

An upper bound for $\|G_k\|_{(H_\nu^1(\mathcal{N}_\infty^\varepsilon))^*}$ results by applying the lemma once more:

$$\begin{aligned} |\langle G_k(t), v \rangle_{(H_\nu^1(\mathcal{N}_\infty^\varepsilon))^* \times H_\nu^1(\mathcal{N}_\infty^\varepsilon)}| &\leq \|v\|_{1,\nu} \|x^k e^{it \cdot x}\|_{0,-\nu} \\ &\leq \|v\|_{1,\nu} C(\hat{\mathcal{N}}, \varepsilon, \nu) \frac{2}{\pi} \left(\frac{2}{\nu}\right)^{\|k\|_1+1} (\|k\|_1 + \mathfrak{D}\mathfrak{H}) \end{aligned}$$

is true for all $v \in H_\nu^1(\mathcal{N}_\infty^\varepsilon)$.

B.4 Proof of Theorem 4

In order to prove analyticity of $t \mapsto \psi(\cdot, t)$ in the strip \mathcal{D}_{ν_2} , it is sufficient to show that

$$\mathcal{D}_{\nu_2} \ni t \mapsto \Psi^\varepsilon(\psi(\cdot, t), v) \in \mathbb{C} \quad (96)$$

is holomorphic for each $v \in H_\nu^1(\mathcal{N}_\infty^\varepsilon)$. Because of theorem 3, for $k \in \{1, 2\}, t \in \mathcal{D}_{\nu_2}$ and $h > 0$ it is

$$\begin{aligned} \Psi^\varepsilon((\partial_{e_k} \psi)(t), v) &= \lim_{h \rightarrow 0} \frac{1}{h} \Psi^\varepsilon(\psi(\cdot, t + he_k) - \psi(\cdot, t), v) \\ &= \lim_{h \rightarrow 0} \frac{1}{h} \langle G(t + he_k) - G(t), v \rangle \\ &= \langle G_{e_k}(t), v \rangle \\ &= \Psi^\varepsilon(\psi_{e_k}(t), v) \end{aligned} \quad (97)$$

for all $v \in H_\nu^1(\mathcal{N}_\infty^\varepsilon)$. The properties of the sesquilinear form Ψ^ε summarized in theorem 2 finally show that $(\partial_{e_k} \psi)(t) = \psi_{e_k}(t)$ in $H_\nu^1(\mathcal{N}_\infty^\varepsilon)$.

The verification of (39) follows from the estimates in of $t \mapsto e^{it \cdot x}$ because

$$\|\psi_k(t)\|_{1,-\nu} \leq \frac{1}{\gamma} \|G_k(t)\|_{(H_\nu^1(\mathcal{N}_\infty^\varepsilon))^*} \quad (98)$$

holds with the inf-sup constant γ .

B.5 Proof of Theorem 5

For fixed $M > 0$ select two sequences of simple functions $\{\hat{F}_M^n : \Omega \rightarrow \mathbb{C}\}, \{\psi_M^n : \Omega \rightarrow \mathbb{C}\}$ respectively, and a collection $\{\Omega_M^{n,j} : j = 0, \dots, J_n\}$ of measurable subsets of Ω_M such that for each $n \in \mathbb{N}$

$$(s1) \quad \Omega_M = \cup_{j=0}^{J_n} \Omega_M^{n,j} \quad \text{and} \quad j_1 \neq j_2 \Rightarrow \Omega_M^{n,j_1} \cap \Omega_M^{n,j_2} = \emptyset$$

$$(s2) \quad \text{for } j = 1, \dots, J_n \text{ and } t_1, t_2 \in \Omega_M^{n,j} \text{ arbitrary}$$

$$\|\psi(\cdot, t_1) - \psi(\cdot, t_2)\|_{1,-\nu} < 2^{-n}$$

$$(s3) \quad \hat{F}_M^n|_{\Omega_M^{n,j}} = \text{const for } j = 0, \dots, J_n$$

$$(s4) \quad |\hat{F}_M^n(t)| \leq |\hat{F}_M(t)| \text{ such that } \hat{F}_M^n(t) \rightarrow \hat{F}_M(t) \text{ as } n \rightarrow \infty \text{ for a.e. } t \in \Omega_M$$

(s5) For arbitrary $t_M^{n,j} \in \Omega_M^{n,j}$ set

$$\psi_M^n(t)|_{\Omega_M^{n,j}} := \psi(\cdot, t_M^{n,j}), \quad \forall j = 1, \dots, J_n.$$

To realize property (s2), the continuity assumption on $\psi(\cdot, t)$ is needed. Whereas $\{\hat{F}_M^n : n \in \mathbb{N}\}$ approximates $\hat{F}_M(t)$ from below, the second collection of simple functions $\{\psi_M^n(\cdot, t) : n \in \mathbb{N}\}$ collocates the continuous function $\psi(\cdot, t)$.

As a consequence

$$\begin{aligned} \|\hat{F}_M(t)\psi(\cdot, t) - \hat{F}_M^n(t)\psi_M^n(\cdot, t)\|_{1,-\nu} &\leq \|\psi(\cdot, t)\|_{1,-\nu} |\hat{F}_M(t) - \hat{F}_M^n(t)| \\ &\quad + |\hat{F}_M^n(t)| 2^{-n} \\ &\leq \frac{C_\nu}{\gamma} |\hat{F}_M(t) - \hat{F}_M^n(t)| + |\hat{F}_M(t)| 2^{-n} \end{aligned}$$

holds for a.e. $t \in \Omega_M$ with the constants γ from (33) and $C_\nu := \|e^{it \cdot x}\|_{(H_\nu^1(\mathcal{N}_\infty^\varepsilon))^*}$. With property (s4) the equation (bi1) follows where $w_M^n(x, t) := \hat{F}_M^n(t)\psi_M^n(x, t)$. Furthermore, the Lebesgue dominated convergence theorem implies (bi2).

B.6 Proof of Theorem 6

Recalling the linear problem (29) for $\psi(x, t)$ in the variational setting (30), the identity

$$\Psi^\varepsilon(u_M^\varepsilon, v) = \lim_{n \rightarrow \infty} \frac{1}{2\pi} \int_{\mathcal{N}_\infty^\varepsilon} \left(\int_{\Omega_M} \sum_{j=1}^{J_n} \hat{F}_M^n(t) e^{it_M^{n,j} \cdot x} \chi_{\Omega_M^{n,j}} \right) \overline{v(x)} \quad (99)$$

is obvious because of the continuity of $u \mapsto \Psi^\varepsilon(u, \cdot)$. The properties (s3) and (s4) of the simple functions constructed in the previous theorem give $|\hat{F}_M^n(t)| \leq |\hat{F}_M(t)|$ for a.e. $t \in \Omega_M$. Therefore

$$|\hat{F}_M^n(x)| := \int_{\Omega_M} |\hat{F}_M^n(t) e^{it_M^{n,j} \cdot x} \chi_{\Omega_M^{n,j}}| dt \leq \int_{\Omega_M} |\hat{F}_M(t)| dt \quad (100)$$

for all $x \in \mathbb{R}^2$. The application of the Lebesgue's theorem on dominated convergence gives

$$\lim_{n \rightarrow \infty} \int_{\mathcal{N}_\infty^\varepsilon} \hat{F}_M^n(x) \overline{v(x)} dD_x = \int_{\mathcal{N}_\infty^\varepsilon} \lim_{n \rightarrow \infty} \hat{F}_M^n(x) \overline{v(x)} dD_x. \quad (101)$$

Since $\hat{F}_M^n(t) \rightarrow \hat{F}_M e^{it \cdot x}$ as $n \rightarrow \infty$ for almost every $t \in \Omega_M$, the Lebesgue's theorem on dominated convergence can be applied once more to obtain

$$\lim_{n \rightarrow \infty} \hat{F}_M^n(x) = \int_{\Omega_M} \lim_{n \rightarrow \infty} \hat{F}_M(t) e^{it \cdot x} dt = 2\pi F_M(x). \quad (102)$$

This completes the proof because it is shown that

$$\Psi^\varepsilon(u_M^\varepsilon, v) = \lim_{n \rightarrow \infty} \frac{1}{2\pi} \int_{\mathcal{N}_\infty^\varepsilon} \hat{F}_M^n(x) \overline{v(x)} dD_x = \int_{\mathcal{N}_\infty^\varepsilon} F_M(x) \overline{v(x)} dD_x \quad (103)$$

holds for all test functions $v \in \mathcal{H}_\nu^1(\mathcal{N}_\infty^\varepsilon)$.

B.7 Proof of Theorem 8

For $k \in \mathbb{Z}^2$ and $\varepsilon > 0$ define

$$\hat{\mathcal{N}}(k, \varepsilon) := \varepsilon(\hat{\mathcal{N}} + \pi k), \quad \hat{Y}(k, \varepsilon) := \varepsilon(\hat{Y} + \pi k). \quad (104)$$

For each $\varepsilon > 0$ there exists a locally finite C^∞ -partition of unity $\{\alpha_k(\cdot, \varepsilon) : k \in \mathbb{Z}^2\}$ associated to $\{\hat{Y}_k(\cdot, \varepsilon) : k \in \mathbb{Z}^2\}$ such that

$$(p1) \quad \alpha_k^\varepsilon \in C^\infty(\mathbb{R}^2)$$

$$(p2) \quad \text{supp } \alpha_k^\varepsilon \subset \hat{Y}(k, \varepsilon)$$

$$(p3) \quad 0 \leq \alpha_k^\varepsilon(x) \leq 1$$

$$(p4) \quad \|\nabla \alpha_k^\varepsilon(x)\| < C(\varepsilon)$$

for all $k \in \mathbb{Z}^2$ and of course

$$(p5) \quad \sum_{k \in \mathbb{Z}^2} \alpha_k^\varepsilon(x) = 1 \quad \forall x \in \mathbb{R}^2.$$

Since Ψ^ε is a continuous sesquilinear form on $H_{-\nu}^1(\mathcal{N}_\infty^\varepsilon) \times H_\nu^1(\mathcal{N}_\infty^\varepsilon)$, for $v \in H_\nu^1(\mathcal{N}_\infty^\varepsilon)$ holds

$$\begin{aligned} \Psi^\varepsilon(\psi, v) &= \sum_{k \in \mathbb{Z}^2} \Psi^\varepsilon(\psi, v_k^\varepsilon) \\ &= \sum_{k \in \mathbb{Z}^2} \int_{\hat{\mathcal{N}}(\varepsilon, k)} A\left(\frac{x}{\varepsilon}\right) D_x\left(\phi\left(\frac{x}{\varepsilon}\right) e^{it \cdot x}\right) \overline{D_x v_k^\varepsilon(x)} \\ &\quad + a\left(\frac{x}{\varepsilon}\right) \phi\left(\frac{x}{\varepsilon}\right) e^{it \cdot x} \overline{v_k^\varepsilon(x)} dD_x, \end{aligned} \quad (105)$$

where $v_k^\varepsilon(x) := \alpha_k^\varepsilon(x)v(x)$ is compactly supported. The goal to reduce the integrals on $\hat{\mathcal{N}}(k, \varepsilon)$ to integrals on the reference network $\hat{\mathcal{N}} = \hat{\mathcal{N}}(0, 1)$ can be achieved by the substitution

$$\frac{x}{\varepsilon} = y + \pi \tilde{k} \quad \text{for } x \in \hat{Y}(k, \varepsilon), \quad (106)$$

with $\tilde{k} \in 2\mathbb{Z}^2$ given by

$$\tilde{k}_j := \begin{cases} k_j, & k_j \text{ even} \\ k_j - 1, & k_j \text{ odd} \end{cases}, \quad j = 1, 2. \quad (107)$$

Taking into consideration the periodicity of A, a and ϕ , each integral in the sum (105) writes

$$\begin{aligned} \int_{\hat{\mathcal{N}}(k - \tilde{k}, 1)} &\left\{ \frac{1}{\varepsilon^2} A(y) D_y(\phi(y) e^{i\varepsilon t \cdot (y + \pi \tilde{k})}) \overline{D_y v_k^\varepsilon(\varepsilon(y + \pi \tilde{k}))} \right. \\ &\left. + a(y) \phi(y) e^{i\varepsilon t \cdot (y + \pi \tilde{k})} \overline{v_k^\varepsilon(\varepsilon(y + \pi \tilde{k}))} \right\} \varepsilon dD_y. \end{aligned} \quad (108)$$

The functions

$$v_k(y, t) := v_{\tilde{k}}^\varepsilon(\varepsilon(y + \pi\tilde{k}))e^{-i\varepsilon t \cdot (y + \pi\tilde{k})}, \quad t \in \mathbb{R}^2, k \in \mathbb{Z}^2, \quad (109)$$

originally only defined for $y \in \text{supp } v_k^\varepsilon(\varepsilon(\cdot + \pi\tilde{k})) \subset \hat{\mathcal{N}}(k - \tilde{k}, 1)$, can be extended 2π -periodically to all $\hat{\mathcal{N}}_\infty$. Because the complex factors $e^{-i\varepsilon t \cdot (y + \pi\tilde{k})}$, $t \in \mathbb{R}^2$ in (109) do not change the functions essentially, it is obvious that $v_k(\cdot, t) \in \mathcal{H}_{per}^1(\hat{\mathcal{N}})$. Using the definition (109), the integrals (108) become

$$\int_{\hat{\mathcal{N}}(k - \tilde{k}, 1)} \left\{ \frac{1}{\varepsilon^2} A(y) D_y(\phi(y) e^{i\varepsilon t \cdot y}) \overline{D_y(v_k(y, t) e^{i\varepsilon t \cdot y})} + a(y) \phi(y) \overline{v_k(y, t)} \right\} \varepsilon dD_y, \quad (110)$$

which is now independent of k . As a consequence, the domain of integration can be replaced by the reference network $\hat{\mathcal{N}}$ and therefore

$$\Psi^\varepsilon(\psi, v) = \sum_{k \in \mathbb{Z}^2} \varepsilon^{-1} \Phi_t^\varepsilon(\phi, v_k). \quad (111)$$

Due to the unique solvability of the unit cell problem (49)

$$\Psi^\varepsilon(\psi, v) = \sum_{k \in \mathbb{Z}^2} \int_{\hat{\mathcal{N}}} \overline{v_k(y, t)} \varepsilon D_y = \int_{\mathcal{N}_\infty^\varepsilon} \bar{v} e^{it \cdot x} dD_x \quad (112)$$

holds for all for all $v \in H_\nu^1(\mathcal{N}_\infty^\varepsilon)$.

References

- [1] I. Babuška, A.K. Aziz, *Survey lectures on the mathematical foundations of the finite element method*, in *The Mathematical Foundations of the Finite Element Method with Applications to Partial Differential Equations*, Academic Press, New York, 1972, 3 – 359
- [2] D. Cioranescu, P. Donato, *An Introduction to Homogenization*, Oxford University Press, Oxford, 1999.
- [3] K. Yosida, *Functional Analysis*, Springer-Verlag, Berlin, New York, 1995.
- [4] A.-M. Matache, I. Babuška, Ch. Schwab, *Generalized p-FEM in homogenization*, Numer. Math.(2000) **86**, 319–375.
- [5] A.-M. Matache, *Spectral and p- Finite Elements for problems with microstructure*, Dissertation, ETH Zürich, 2000.
- [6] R.C. Morgan, I. Babuška, *An approach for constructing families of homogenized equations for periodic media. I: An integral representation and its consequences*, SIAM J. Math. Anal. (1991) **22**, 1–15.

- [7] A.W. Rüegg, *Implementation of Generalized Finite Element Methods for Homogenization Problems*, Journal of Scientific Computing, (2002) **17**, 671–681
- [8] B. Szabo, I. Babuška, *Finite Element Analysis*, John Wiley & Sons, New York, 1991.

Research Reports

No.	Authors	Title
02-23	A.W. Rüegg, A. Schneebeli, R. Lauper	Generalized <i>hp</i> -FEM for Lattice Structures
02-22	L. Filippini, A. Toselli	<i>hp</i> Finite Element Approximations on Non-Matching Grids for the Stokes Problem
02-21	D. Schötzau, C. Schwab, A. Toselli	Mixed <i>hp</i> -DGFEM for incompressible flows II: Geometric edge meshes
02-20	A. Toselli, X. Vasseur	A numerical study on Neumann-Neumann and FETI methods for <i>hp</i> -approximations on geometrically refined boundary layer meshes in two dimensions
02-19	D. Schötzau, Th.P. Wihler	Exponential convergence of mixed <i>hp</i> -DGFEM for Stokes flow in polygons
02-18	P.-A. Nitsche	Sparse approximation of singularity functions
02-17	S.H. Christiansen	Uniformly stable preconditioned mixed boundary element method for low-frequency electromagnetic scattering
02-16	S.H. Christiansen	Mixed boundary element method for eddy current problems
02-15	A. Toselli, X. Vasseur	Neumann-Neumann and FETI preconditioners for <i>hp</i> -approximations on geometrically refined boundary layer meshes in two dimensions
02-14	Th.P. Wihler	Locking-Free DGFEM for Elasticity Problems in Polygons
02-13	S. Beuchler, R. Schneider, C. Schwab	Multiresolution weighted norm equivalences and applications
02-12	M. Kruzik, A. Prohl	Macroscopic modeling of magnetic hysteresis
02-11	A.-M. Matache, C. Schwab, T. von Petersdorff	Fast deterministic pricing of options on Lévy driven assets
02-10	D. Schötzau, C. Schwab, A. Toselli	Mixed <i>hp</i> -DGFEM for incompressible flows
02-09	Ph. Frauenfelder, Ch. Lage	Concepts - An object-oriented software package for partial differential equations
02-08	A.-M. Matache, J.M. Melenk	Two-Scale Regularity for Homogenization Problems with Non-Smooth Fine Scale Geometry
02-07	G. Schmidlin, C. Lage, C. Schwab	Rapid solution of first kind boundary integral equations in \mathbb{R}^3